IAI Journals.ASM.org

Cyclic di-GMP Modulates Gene Expression in Lyme Disease Spirochetes at the Tick-Mammal Interface To Promote Spirochete Survival during the Blood Meal and Tick-to-Mammal Transmission

Melissa J. Caimano,[a,b,c] Star Dunham-Ems,[a] Anna M. Allard,[a] Maria B. Cassera,[d] Melisha Kenedy,[e] Justin D. Radolf[a,b,c,f,g]

Departments of Medicine,[a] Pediatrics,[b] Molecular Biology and Biophysics,[c] Genetics and Genomic Sciences,[f] and Immunology,[g] University of Connecticut Health Center, Farmington, Connecticut, USA; Department of Biochemistry and Center for Drug Discovery, Virginia Tech, Blacksburg, Virginia, USA[d]; Department of Microbiology and Immunology, University of Oklahoma College of Medicine, Oklahoma City, Oklahoma, USA[e]

***Borrelia burgdorferi*, the Lyme disease spirochete, couples environmental sensing and gene regulation primarily via the Hk1/Rrp1 two-component system (TCS) and Rrp2/RpoN/RpoS pathways. Beginning with acquisition, we reevaluated the contribution of these pathways to spirochete survival and gene regulation throughout the enzootic cycle. Live imaging of *B. burgdorferi* caught in the act of being acquired revealed that the absence of RpoS and the consequent derepression of tick-phase genes impart a Stay signal required for midgut colonization. In addition to the behavioral changes brought on by the RpoS-off state, acquisition requires activation of cyclic di-GMP (c-di-GMP) synthesis by the Hk1/Rrp1 TCS; *B. burgdorferi* lacking either component is destroyed during the blood meal. Prior studies attributed this dramatic phenotype to a metabolic lesion stemming from reduced glycerol uptake and utilization. In a head-to-head comparison, however, the *B. burgdorferi* Δ*glp* mutant had a markedly greater capacity to survive tick feeding than *B. burgdorferi* Δ*hk1* or Δ*rrp1* mutants, establishing unequivocally that glycerol metabolism is only one component of the protection afforded by c-di-GMP. Data presented herein suggest that the protective response mediated by c-di-GMP is multifactorial, involving chemotactic responses, utilization of alternate substrates for energy generation and intermediary metabolism, and remodeling of the cell envelope as a means of defending spirochetes against threats engendered during the blood meal. Expression profiling of c-di-GMP-regulated genes through the enzootic cycle supports our contention that the Hk1/Rrp1 TCS functions primarily, if not exclusively, in ticks. These data also raise the possibility that c-di-GMP enhances the expression of a subset of RpoS-dependent genes during nymphal transmission.**

Borrelia burgdorferi, the causative agent of Lyme disease, is maintained in nature within an enzootic cycle that involves an arthropod vector and vertebrate reservoir hosts, typically, small rodents and birds (1). In the northeastern United States, the primary vector for *B. burgdorferi* is the black-legged deer tick, *Ixodes scapularis* (2, 3). Because *B. burgdorferi* cannot be passaged transovarially, naive larvae acquire spirochetes by feeding on infected reservoir hosts. Successful colonization of the vector requires *B. burgdorferi* to establish an intimate association with rapidly differentiating, highly endocytic midgut epithelial cells (4–6). In order to accomplish this feat, spirochetes must resist deleterious substances within the midgut lumen, such as host- and tick-derived innate immune effector molecules, reactive oxygen species (ROS), and salivary enzymes imbibed from the feeding site (4, 7–11). At the same time, *B. burgdorferi* also must alter its metabolic machinery to exploit the availability of alternative carbon sources (e.g., glycerol, *N*-acetylglucosamine [GlcNAc], chitobiose) as the supply of ingested glucose diminishes (12–15). During nymphal transmission, spirochetes are almost certainly subjected to the same, and potentially additional, blood meal-associated stressors encountered during larval acquisition. Whereas spirochetes are confined to the midgut during acquisition, during transmission, organisms traverse the organ en route to a new mammalian host (5, 6, 16). The larval and nymphal blood meals therefore evoke marked differences in spirochete behavior while eliciting ostensibly similar protective and physiological adaptations.

Throughout its enzootic cycle, *B. burgdorferi* couples environmental sensing with differential gene expression primarily using two two-component systems (TCSs), Hk1/Rrp1 and Hk2/Rrp2, and three σ factors, the housekeeping RpoD and the alternate σ factors RpoN and RpoS (1, 17). Although the contribution of the Hk2 sensor kinase to phosphorylation of the response regulator Rrp2 remains uncertain (18), phosphorylated Rrp2 acts in concert with the DNA-binding Fur ortholog BosR to promote the RpoN-dependent transcription of *rpoS* at the onset of the nymphal blood meal (1, 17). Recently, we reported that a *B. burgdorferi* Δ*rpoS* mutant is unable to exit the midguts of feeding nymphs, while spirochetes lacking *ospC*, the prototypical RpoS-dependent gene, could be recovered from the bite site, establishing unequivocally that RpoS-dependent gene products other than OspC are required for tick-to-mammal transmission (19). Within the mammal, *rpoS* is absolutely required to establish infection (20–23). While the

Received 10 March 2015 **Returned for modification** 9 April 2015
Accepted 11 May 2015

Accepted manuscript posted online 18 May 2015

Citation Caimano MJ, Dunham-Ems S, Allard AM, Cassera MB, Kenedy M, Radolf JD. 2015. Cyclic di-GMP modulates gene expression in Lyme disease spirochetes at the tick-mammal interface to promote spirochete survival during the blood meal and tick-to-mammal transmission. Infect Immun 83:3043–3060. doi:10.1128/IAI.00315-15.

Editor: A. J. Bäumler

Address correspondence to Melissa J. Caimano, mcaima@uchc.edu.

Supplemental material for this article may be found at http://dx.doi.org/10.1128/IAI.00315-15.

doi:10.1128/IAI.00315-15

role of RpoS during chronic infection has not been extensively studied, transcriptional and serological data suggest that at least some RpoS-dependent genes are expressed during later stages of mammalian infection (24–29). Following acquisition, *B. burgdorferi* expresses little to no *rpoS*, permitting transcription of σ^{70}-dependent tick-phase genes (e.g., *ospA*, *bba62*, and the *glp* operon) that are repressed by RpoS within the mammal (12, 19, 24, 30–33). Collectively, these data led us to propose that RpoS acts as a gatekeeper for the reciprocal expression of genes involved in the mammalian and arthropod phases of the enzootic cycle (19, 24). In contrast, *B. burgdorferi*'s other primary regulatory pathway, the Hk1/Rrp1 TCS, is dispensable for mammalian infection and appears to function exclusively within ticks (34–36). Activation of this TCS, which signals via cyclic di-GMP (c-di-GMP), is required for tick midgut colonization. Spirochetes lacking either the sensor kinase Hk1 or the response regulator Rrp1, a diguanylate cyclase (37), are rapidly destroyed during the blood meal (34–36). An important distinction between the Hk1/Rrp1 TCS and Rrp2/RpoN/RpoS pathway (referred to henceforth as the "RpoS pathway") is that the former is active during both acquisition and transmission (34, 35), whereas the latter is on only during transmission (19, 23, 24, 27, 38).

Here, we reevaluated the contribution of c-di-GMP signaling to spirochete survival and gene regulation throughout the enzootic cycle. Confocal live imaging of *B. burgdorferi* caught in the act of being acquired revealed that the derepression of tick-phase genes associated with the RpoS-off state imparts a Stay signal required to colonize the tick midgut. Using a combination of ultra-performance liquid chromatography (UPLC) in tandem with mass spectrometry (MS) and quantitative reverse transcription-PCR (qRT-PCR), we demonstrated that Hk1 is the cognate histidine kinase for Rrp1 and that the response regulator Rrp1 is the sole source of c-di-GMP during cultivation *in vitro*. In accord with prior studies (34–36), we confirmed that both Hk1 and Rrp1 are required for the survival of *B. burgdorferi* during the acquisition and transmission blood meals. Prior studies by He et al. (35) attributed the survival defect of Rrp1-deficient *B. burgdorferi* to a metabolic lesion brought on by reduced expression of the c-di-GMP-dependent *glp* operon (*bb0240-bb0243*) involved in glycerol uptake and utilization (35). In our head-to-head comparison, however, the *B. burgdorferi* Δ*glp* mutant displayed markedly increased survival in feeding larvae than *B. burgdorferi* Δ*hk1* and Δ*rrp1* mutants. Moreover, unlike *B. burgdorferi* Δ*hk1*- and Δ*rrp1*-infected nymphs, *B. burgdorferi* Δ*glp*-infected nymphs transmitted infection to naive mice. Collectively, these results demonstrate unequivocally that glycerol utilization is only one component of the protection afforded by c-di-GMP signaling. Genome-wide transcriptional profiling of *B. burgdorferi* wild-type (WT) and Δ*rrp1* mutant strains by transcriptome sequencing (RNA-Seq) suggests that the tick-adaptive response mediated by c-di-GMP is multifactorial, involving (i) remodeling of the cell envelope as a means of defending spirochetes against threats engendered during the blood meal, (ii) utilization of alternate substrates for energy generation and biosynthesis of intermediary metabolites, and (iii) chemotactic responses. The results of expression profiling of c-di-GMP-regulated genes through the enzootic cycle support our contention that the Hk1/Rrp1 TCS functions primarily, if not exclusively, in ticks. Lastly, our data also raise the possibility that c-di-GMP enhances the expression of a subset of RpoS-dependent genes during nymphal transmission.

MATERIALS AND METHODS

Ethics statement. Animal protocols described in this work strictly follow the recommendations of the *Guide for the Care and Use of Laboratory Animals* of the National Institutes of Health (136) and were approved by the University of Connecticut Health Center Animal Care Committee under the auspices of Animal Welfare Assurance A347-01.

Culture and maintenance of bacterial strains. *B. burgdorferi* isolates (see Table S1 in the supplemental material) were cultivated in modified Barbour-Stoenner-Kelly II (BSK-II) medium (39) supplemented with 6% rabbit serum (Pel-Freeze Biologicals, Rogers, AR) and antibiotics where appropriate. Strain Bb1286 was generated from wild-type strain *B. burgdorferi* B31 5A4 NP1 (40) by electroporation (41) with the suicide plasmid pMC2498 to insert a P_{flaB}-*gfp* P_{flgB}-*aacC1* cassette into the endogenous cp26 plasmid (42). B31 5A4 NP1 Δ*rrp1* (Bb1520) and Δ*plzA* (Bb1548) mutants were generated by insertional inactivation using previously described constructs (43, 44). The plasmid content of all isolates was monitored as previously described (45). For temperature shift experiments, *B. burgdorferi* isolates were cultivated to mid-logarithmic phase (~1×10^7 to 3×10^7 spirochetes per ml) in BSK-II medium at 23°C and then transferred to fresh medium at a density of 10^5 spirochetes per ml. Following the temperature shift, the cultures were maintained at 37°C until late logarithmic phase (~7×10^7 to 1×10^8 spirochetes per ml). *Escherichia coli* strains were maintained in lysogeny broth (LB) with the appropriate antibiotic. Selection of *E. coli* strains was performed on LB agar (LB with 1.5% agar) plates supplemented with the appropriate antibiotic.

DNA manipulations and routine cloning. Routine and high-fidelity PCR amplification reactions were performed using Choice *Taq* (Denville Scientific, Metuchen, NJ) and TaKaRa *Ex Taq* (Fisher Scientific, Pittsburgh, PA) DNA polymerase, respectively. Routine molecular cloning and plasmid propagation were performed using *E. coli* TOP10 cells (Life Technologies, Grand Island, NY). Plasmid DNAs were purified using Qiagen Midi and Spin Prep kits (Qiagen, Valencia, CA). Nucleotide sequencing was performed by Agencourt/Beckman Genomics (Danvers, MA).

SDS-PAGE and immunoblot analyses. Whole-cell lysates were prepared from spirochetes cultivated *in vitro* following a temperature shift from 23°C to 37°C as described above. Equivalent amounts of lysate (~2×10^7 spirochetes per ml) were separated on 12.5% separating polyacrylamide minigels, and the proteins were visualized by silver staining. For immunoblotting, proteins were transferred to nylon-supported nitrocellulose and incubated with rat polyclonal antiserum against FlaB (46), GlpD (12), OspC, OspA, and Rrp1, followed by goat anti-rat horseradish peroxidase-conjugated secondary antibody (Southern Biotechnology Associates, Birmingham, AL). Monospecific polyclonal antisera against strain B31 OspC, OspA, and Rrp1 (43) were generated in female Sprague-Dawley rats (weight, 150 to 174 g) using the corresponding recombinant histidine-tagged protein, as previously described (47). Immunoblots were developed using the SuperSignal West Pico chemiluminescence substrate (Pierce, Rockford, IL).

Acquisition of *B. burgdorferi* by larvae and nymphs. To generate naturally infected larvae and nymphs for acquisition studies, 3- to 5-week-old female C3H/HeJ mice (purchased from Jackson Laboratories, Bar Harbor, ME, or NCI—Frederick National Laboratory for Cancer Research/APA, Frederick, MD) were inoculated intradermally with 1×10^4 temperature-shifted organisms. Infection was confirmed at 2 and 4 weeks postinoculation by serology and cultivation of ear tissue specimens in BSK-II medium containing antibiotic cocktail (0.05 mg/ml sulfamethoxazole, 0.02 mg/ml phosphomycin, 0.05 mg/ml rifampin, 0.01 mg/ml trimethoprim, 0.0025 mg/ml amphotericin B) to minimize contamination. Additional antibiotics (0.05 mg/ml gentamicin, 0.05 mg/ml streptomycin, and/or 0.4 mg/ml kanamycin) were added where appropriate. Cultures were monitored for spirochetes weekly by dark-field microscopy. Infected mice were used as a blood meal source for pathogen-free *I.*

scapularis larvae (Oklahoma State University, Stillwater, OK) and nymphs (generated in-house by feeding larvae on naive mice). Larvae (200 to 300 per mouse) were infected by whole-body infestation of syringe-inoculated mice, while naive nymphs (15 to 20 per mouse) were confined to a capsule affixed to the shaved back of an infected mouse, as previously described (38). Larvae and naive nymphs were allowed to feed for designated time points postplacement. To generate infected nymphs for transmission studies, larvae fed to repletion on infected C3H/HeJ mice were held over saturated potassium sulfate in an environmental incubator until they had molted.

Transmission by nymphs infected with wild-type *B. burgdorferi*. Transmission by unfed (flat) nymphs that had been naturally infected (as larvae) or infected by immersion was assessed using 15 to 20 nymphs per mouse confined to a capsule affixed to the backs of naive C3H/HeJ mice as previously described (38). Nymphs were allowed to feed for the time points designated below, typically 72 to 96 h postplacement.

Assessment of spirochete burdens within *I. scapularis* larvae and nymphs by qPCR. Spirochete burdens (i) during acquisition using individual pools of 15 larvae or 3 nymphs that had fed to repletion on a syringe-inoculated mouse (3 mice per group) and (ii) during transmission using triplicate pools of five *B. burgdorferi*-infected nymphs fed to repletion on naive C3H/HeJ mice were assessed by qPCR. Total genomic DNA was isolated from *B. burgdorferi*-infected ticks using a Gentra Puregene yeast/bacteria kit (Qiagen) according to the manufacturer's instructions. DNAs were diluted 1:10 in water prior to being analyzed by quantitative PCR (qPCR) using a TaqMan-based assay for *flaB* (see Table S1 in the supplemental material) (38). Spirochete burdens were assessed in at least three independent experiments.

qRT-PCR. Total RNA was isolated from pools of (i) ~100 larvae or ~25 nymphs fed to repletion on C3H/HeJ mice that had been syringe inoculated with *B. burgdorferi* wild-type isolate CE162 or Bb1286 (acquisition) and (ii) ~20 to 25 unfed *B. burgdorferi*-infected unfed nymphs fed to repletion on a naive C3H/HeJ mouse (transmission) as previously described (38). cDNAs that had and had not undergone reverse transcription were assayed in quadruplicate using iQ Supermix (Bio-Rad) and the primer pairs described in Table S1 in the supplemental material. *flaB*-normalized copy number values were compared within Prism software (v5.00; GraphPad Software, San Diego, CA) using an unpaired *t* test with two-tailed *P* values and the 95% confidence interval.

Processing of nymphal midguts for microscopy. Intact midguts were isolated from Bb914-infected nymphs at 72 h postplacement and labeled with FM4-64 (2 ng/ml in phosphate-buffered saline [PBS]; Life Technologies) as described previously (6). Epifluorescence microscopy was performed on an Olympus BX41 microscope equipped with a Retiga Exi camera (QImaging, Surrey, British Columbia, Canada); images were acquired using a 40× (numerical aperture, 1.4) oil immersion objective with QCapture software (v2.1; QImaging). Nymphal midguts were processed for confocal imaging as previously described (6). Confocal microscopy was performed on a Zeiss LSM-510 microscope (Carl Zeiss Microscopy, LLC, Thronwood, NY); serial Z-series images were acquired in both the red and green channels (6). Briefly, Z-series images were acquired as 1-μm optical sections through a single epithelial layer (i.e., from the basement membrane toward the lumen; see Fig. 2A for a schematic) along the longitudinal plane. The midway point for each specimen was determined during image processing on the basis of the thickness of the epithelium. A minimum of 18 nymphal midguts each were examined during acquisition and transmission.

Measurement of c-di-GMP levels. Cultures (50 ml each) of the WT B31 5A4 NP1 (Bb1399), Δ*hk1* (Bb1197), and Δ*rrp1* (Bb1451) isolates were grown, in triplicate, to late logarithmic phase following a temperature shift. Cells were harvested by centrifugation at 8,000 × *g* for 15 min at 4°C, transferred to a preweighed, clean, 50-ml conical tube using 1 ml ice-cold PBS, and pelleted as described above. Pellets were resuspended in 30 ml of 0.19% ice-cold formaldehyde and centrifuged as described above. After all of the supernatant was carefully removed, the net weight of each pellet was recorded. The pellets were resuspended in 0.5 ml of PCR-grade water and transferred to a 4-ml snap-cap tube. Samples were boiled for 10 min and then placed on ice. Ice-cold 99% ethanol (1.25 ml) was added to each tube, and samples were kept on ice for 30 min. Cell material was pelleted by centrifugation at 9,000 × *g* for 10 min at 4°C, and the supernatant was transferred to a clean tube. The pellet was resuspended in 1.5 ml of ice-cold 70% ethanol, incubated on ice for 30 min, and then centrifuged at 9,000 × g for 10 min at 4°C. The combined supernatants were filtered through a 0.22-μm-pore-size syringe filter and stored at −80°C. c-di-GMP was detected by ultraperformance liquid chromatography (UPLC) in tandem with mass spectrometry (MS) using an Acquity UPLC system coupled to an Acquity TQD mass spectrometer (Waters Corporation). The separation of c-di-GMP was achieved using an ion-pairing reversed-phase UPLC method (48). Briefly, the eluent system was composed of 1.25 mM dibutylammonium acetate in 10 mM ammonium formate (pH 5.0) (eluent A) and 1.25 mM dibutylammonium acetate in acetonitrile (eluent B) with a gradient of 100% eluent A to 10% eluent B from 2 to 10 min, to 30% eluent B from 10 to 11 min, and back to 100% eluent A at a flow rate of 0.3 ml min^{-1}. An Acquity HSS T3 column (2.1 by 100 mm; particle size, 1.8 μm; Waters) and an Acquity column in-line filter were used. The column and autosampler were maintained at 40°C and 10°C, respectively. Detection of c-di-GMP was performed in electrospray ionization (ESI) negative-ion mode using the multiple-reaction monitoring mode. For ESI-MS/MS analysis, the following ion transition, cone voltage (CV), and collision energy (CE) were used: c-di-GMP *m/z* 689.32 (precursor ion) and 149.99 (product ion); CV, 66 V; and CE, 56 eV. The ESI capillary voltage was 0.3 kV, the source temperature was set at 150°C, and the desolvation temperature was set at 400°C. The flow rate of the desolvation gas (N_2) was set at 600 liters/h. Data acquisition and analysis were carried out with MassLynx (v4.1) and QuanLynx software. The concentration of c-di-GMP was calculated by interpolation of the observed analyte peak area with the corresponding calibration curve and then normalized to the cell pellet wet weight for each sample. Three biological replicates for each strain were assayed per experiment. All three strains were examined in two independent experiments.

Comparison of viability of the Δ*hk1*, Δ*rrp1*, and Δ*glp* isolates in replete larvae infected by immersion. The viability of the B31 5A4 NP1 (Bb1399), Δ*hk1* (Bb1197), Δ*rrp1* (Bb1451), and Δ*glp* (Bb1452) isolates in larvae infected by the immersion method was assessed (49). Briefly, ~200 naive larvae were mixed end over end in a high-density suspension (2×10^8 spirochetes/ml) of each isolate for 1 to 2 h at room temperature. Following immersion, the larvae were washed twice with 1 ml of sterile PBS and allowed to recover overnight in an environmental incubator prior to being fed to repletion on a naive C3H/HeJ mouse. Replete larvae were collected daily over water and were processed for qRT-PCR as described above. Pools of 12 larvae per isolate were processed for immunofluorescence using fluorescein isothiocyanate (FITC)-conjugated anti-*Borrelia* antibody (Kirkegaard & Perry Laboratories, Gaithersburg, MD) as previously described (38). Mice used as a blood meal source for immersion-fed larvae were tested for infection by ear biopsy specimen serology at 4 weeks postinfestation. All four isolates were compared in at least two independent experiments. Following the molt, nymphs were tested for their ability to transmit infection to naive mice (2 to 3 mice per group) using the capsule method described above.

Comparative RNA-Seq analysis of *B. burgdorferi* wild-type and Δ*rrp1* strains. Total RNAs were prepared from *B. burgdorferi* WT and Δ*rrp1* strains (three biological replicates per strain) grown to late logarithmic phase following a temperature shift in BSK-II medium as previously described (34). RNA integrity was checked by use of an Experion RNA chip (Bio-Rad) and qRT-PCR for *flaB*. Prior to library construction, rRNA was removed from each pooled sample using a Ribo-Zero rRNA removal core kit (Epicentre, Madison, WI). Paired-end Illumina TruSeq libraries were generated as previously described (50). Postrun data analyses were performed by the use of the RNA-Rocket program (http://rnaseq.pathogenportal.org/) (51). High-quality reads (*Q* score ≥ 30)

were mapped using the strain B31 RefSeq reference genome (http://patricbrc.org). Mapping, quartile normalization, fold regulation, and significance were determined using the prokaryotic single-end analysis and differential expression analysis options. Reads matching more than one location within the B31 reference genome were excluded during the initial mapping step, which resulted in some highly conserved, paralogous genes carried by plasmids being assigned a read count of zero for both the wild-type and mutant isolates. A gene was considered differentially expressed if (i) the mean number of normalized reads for that gene differed by ≥2-fold compared to that for the wild type and (ii) the difference in expression between the WT and the Δ*rrp1* isolate had a false discovery rate (FDR)-adjusted *P* value (*q* value) of ≤0.05.

Bioinformatics. Routine and comparative sequence analyses were performed using MacVector software (v10.1, MacVector, Inc., Cary, NC). Conserved domain searches were performed using a search of the Conserved Domain Database either alone (http://www.ncbi.nlm.nih.gov/Structure/cdd/cdd.shtml) or within the NCBI Basic Local Alignment Search Tool (BLAST). Candidate surface-exposed lipoproteins within the Rrp1 regulon were identified using the database created by Setubal et al. (52). Candidate outer membrane (OM) proteins (OMPs) were identified using a series of computational programs that predict either OM localization or β-barrel topology. The 1,640 protein-coding sequences of the *B. burgdorferi* genome were analyzed by the use of six computational programs: CELLO (53), pSORTb (54), HHOMP (55), BOMP (56), Pred-TMBB (57), and TMBETADISC-AAC (58). Proteins were considered candidate OMPs if three of six computational programs predicted the protein to be localized to the OM and/or to form a β barrel. The list of candidate OMPs was further refined by removing sequences that were (i) predicted to be lipoproteins (52), (ii) predicted to contain transmembrane α helices by the TMHMM (59) and Phobius (60) programs, or (iii) orthologous to non-OMPs. Finally, the N-terminal region of each candidate OMP sequence was analyzed using the programs SignalP (v3.0) (61), PrediSi (62), and Signal-CF (63) to verify that all potential OMPs were predicted to have a cleaved signal sequence. Protein sequences were also manually inspected for signal sequences using hydrophilicity plots according to the methods of Kyte and Doolittle (64). Proteins predicted to lack a signal sequence by at least one method were excluded from the list of potential OMPs.

RESULTS

The RpoS-off state during acquisition promotes superficial association of *B. burgdorferi* with tick midgut epithelial cells. Previously, we used confocal fluorescence microscopy of strain Bb914, a virulent strain of *B. burgdorferi* wild-type strain 297 expressing green fluorescent protein (GFP), to investigate *B. burgdorferi*-tick interactions during nymphal transmission (6, 19). Results from these imaging studies revealed that spirochetes disseminate through the midgut in two stages: an initial adherence-mediated migration phase during which nonmotile organisms form extensive networks on the surfaces of midgut epithelial cells, followed by a motile phase in which individual spirochetes penetrate the midgut and enter the hemocoel. Extensive characterization of *B. burgdorferi* 297 wild-type and Δ*rpoS* strains in feeding nymphs revealed that RpoS is required for physiological adaptation to the blood meal, network formation, and/or migration out of the midgut during transmission (19). Once in the mammal, spirochetes continue to express *rpoS* but are thought to transition from the RpoS-on state to the RpoS-off state during acquisition (24, 30, 31, 38, 42, 65, 66). Given how little is known about the *B. burgdorferi*-tick interactions involved in acquisition, we reasoned that comparable imaging of spirochetes within acquiring ticks could provide valuable insight into how *B. burgdorferi*'s genetic programs influence spirochete behavior during this stage of the enzootic cycle. We opted to use Bb914 for these acquisition studies because this strain has already been extensively characterized by confocal microscopy in nymphs during transmission and infected murine tissues (6, 19, 67–69). The intense autofluorescence of the tick cuticle necessitates the removal of intact midguts prior to examination by fluorescence microscopy (6, 19), a procedure that is virtually impossible to perform on feeding larvae. Therefore, for these imaging studies, we used naive nymphs as surrogates for larvae. Consistent with findings presented in previously published reports (31, 34, 70, 71), *I. scapularis* nymphs readily acquire *B. burgdorferi* (Fig. 1A); the high spirochete burdens in acquiring nymphs (3.04-fold; $P = 0.0008$) compared to larvae is not surprising, given the larger volumes of blood imbibed. Hemolymph collected from acquiring nymphs ($n = 115$) at 72 h postplacement was uniformly culture negative, indicating that spirochetes did not penetrate the midgut. By comparison, the rate of culture positivity of hemolymph collected from transmitting nymphs ($n = 62$) at the same time point was ~90% (19). Using primers specific for RpoS-upregulated genes (*ospC* and *dbpA*) and RpoS-repressed genes (*ospA*, *bb0240* [*glpF*], *bba62* [*lp6.6*], and *bba74*), we confirmed that the expression profiles of *B. burgdorferi* in acquiring nymphs mirrored those of spirochetes within replete larvae (Fig. 1B).

We next used wide-field and confocal fluorescence microscopy to compare the behavior of *B. burgdorferi* in acquiring and transmitting nymphs at 72 h postplacement, the time point during transmission when spirochetes form networks and traverse the midgut (6, 19, 65, 72). When viewing images of fed midguts at this late stage of feeding, one must be cognizant of the fact that the epithelial surface is highly irregular and that the lumen is crowded with hypertrophied and detached midgut digestive cells (4, 73, 74) (see the cartoon in Fig. 2A). By epifluorescence microscopy of whole-mount midguts (Fig. 2B), spirochetes within acquiring nymphs were confined exclusively to the luminal surfaces of the epithelium and the open spaces between protuberant digestive cells. In contrast, spirochetes in transmitting nymphs formed confluent networks that penetrated the full thickness of the epithelium and, in some cases, reached the basement membrane (Fig. 2B, Transmission, arrows). By confocal microscopy (Fig. 2C), spirochetes in acquiring nymphs followed the contours of the epithelial cell surfaces without entering the intercellular spaces; no organisms were observed at or near the basement membrane. In transmitting nymphs, spirochetes penetrated the entire epithelial layer (arrows in Fig. 2C indicate spirochetes in proximity to the basement membrane).

Hk1 and Rrp1 function cooperatively to promote synthesis of c-di-GMP and expression of c-di-GMP-dependent genes. Spirochetes lacking either the sensory histidine kinase Hk1 (34) or its putative response regulator, Rrp1 (35, 36), are destroyed within the midguts of larvae and nymphs during the blood meal. The survival of *B. burgdorferi* Δ*hk1* and Δ*rrp1* mutants in feeding ticks was restored to wild-type levels by complementation with a wild-type copy of the corresponding gene (34, 35). Although the survival defects of the *B. burgdorferi* Δ*hk1* and Δ*rrp1* mutants are indistinguishable (34–36), at present, there is no direct evidence establishing that these components function cooperatively to promote the synthesis of c-di-GMP. We therefore used ultraperformance liquid chromatography in tandem with mass spectrometry (48) to compare the intracellular levels of c-di-GMP in the *B. burgdorferi* wild-type, Δ*hk1*, and Δ*rrp1* strains cultivated *in vitro*.

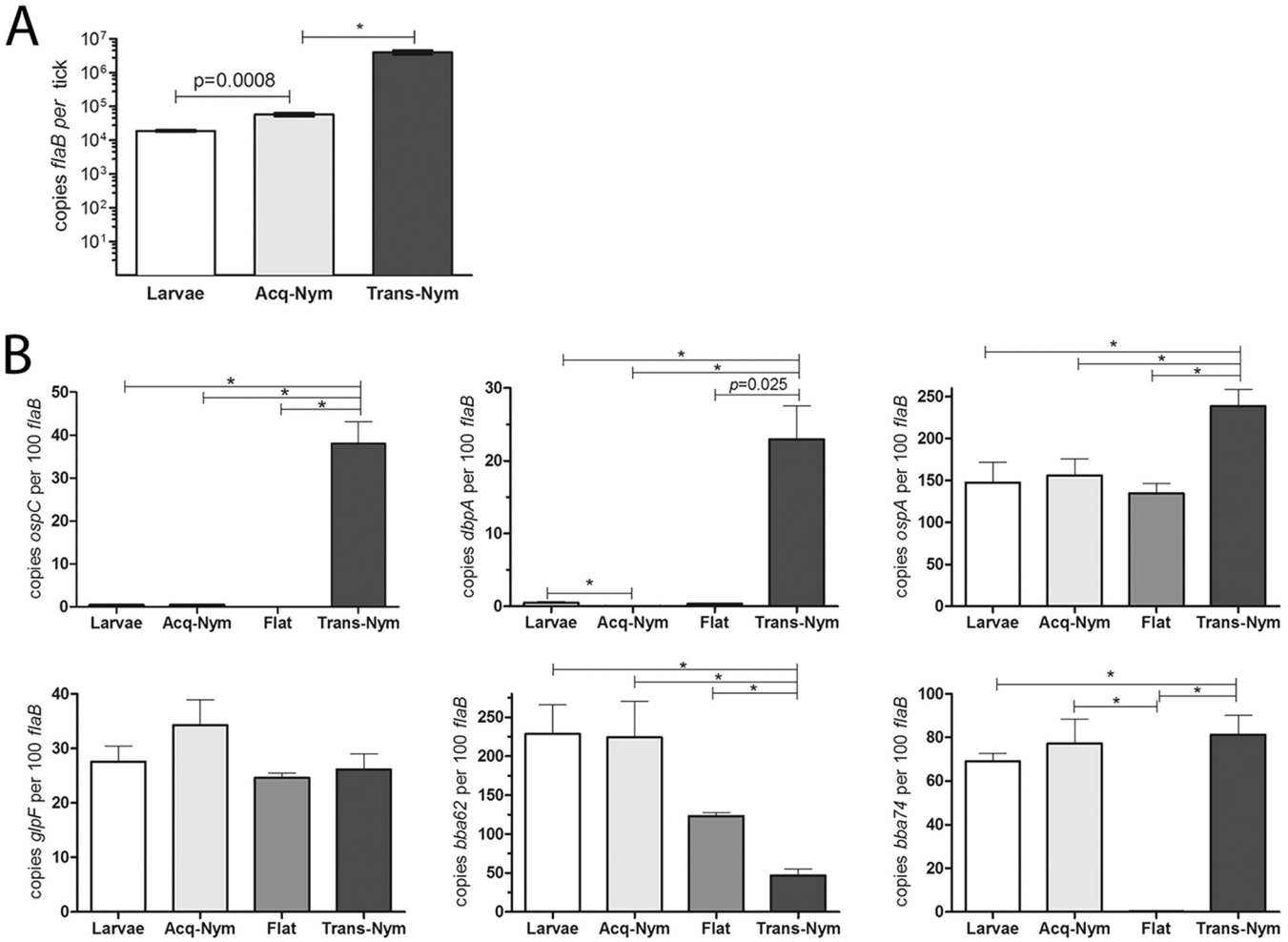

FIG 1 Spirochetes acquired by naive nymphs are in an RpoS-off state. (A) Spirochete burdens in larvae and acquiring nymphs (Acq-Nym) fed on C3H/HeJ mice infected with wild-type strain 297 (CE162) compared to those in infected transmitting nymphs (Trans-Nym) fed on a naive mouse. Genome copy numbers were assessed by qPCR using a TaqMan-based assay for *flaB*. Values represent the average number of *flaB* copies per tick ± SEM from at least three biologically independent experiments. (B) Transcript levels for prototypical RpoS-upregulated (*ospC* and *dbpA*) and -repressed (*ospA*, *bb0240* [*glpF*], *bba74*, and *bba62*) genes in replete larvae and acquiring and transmitting nymphs at 72 h postplacement compared to those in unfed (Flat) nymphs. Values represent the average copy number ± SEM normalized per 100 copies of *flaB*. Statistical significance ($P \leq 0.05$) was determined using an unpaired *t* test. *, $P \leq 0.0001$.

As shown in Fig. 3A, we detected essentially no c-di-GMP in lysates prepared from *B. burgdorferi* Δ*rrp1*, a finding which is consistent with Rrp1 being the sole diguanylate cyclase in *B. burgdorferi* (37). We also detected significantly ($P < 0.05$) lower levels of c-di-GMP in the *B. burgdorferi* Δ*hk1* mutant (Fig. 3A), further supporting the notion that Hk1 is the cognate sensor kinase for Rrp1. Furthermore, we confirmed that Hk1, like Rrp1 (35, 43), is required for expression of the *glp* operon (*bb0240-bb0243*). By qRT-PCR and immunoblotting, both *B. burgdorferi* Δ*hk1* and Δ*rrp1* mutants expressed markedly reduced levels of *bb0240* (*glpF*) and BB0243/GlpD, respectively (Fig. 3B and C). *ospA*, like the *glp* operon, is transcribed by σ^{70} and repressed by RpoS within the mammalian host (12, 19, 24). Thus, it was of interest to determine whether expression of *ospA* also is upregulated by c-di-GMP. As shown in Fig. 3C and D, respectively, *ospA* protein and transcript were expressed at wild-type levels in the *B. burgdorferi* Δ*hk1* and Δ*rrp1* mutants.

c-di-GMP mediates a tick-adaptive survival program that involves genes outside the *glp* operon. Previously, He et al. (35) attributed the decreased survival of *B. burgdorferi* Δ*rrp1* to the loss of *glp* gene expression. However, constitutive high-level expression of the *glp* operon only partially restored the survival of the *B. burgdorferi* Δ*rrp1* mutant in feeding ticks (35). Moreover, we reported (12) that *B. burgdorferi* lacking BB0243/GlpD, a glycerol-3-dehydrogenase, is acquired by larvae at wild-type levels and exhibits only a modest (3.5- to 5-fold) reduction in spirochete burdens during transmission. We reasoned, therefore, that a side-by-side comparison of *B. burgdorferi* wild-type, Δ*hk1*, Δ*rrp1*, and Δ*glp* isolates would more rigorously assess the extent to which *glp* gene products contribute to survival and transmissibility in feeding ticks. Because the *B. burgdorferi* Δ*glp* isolate (Bb1452) used for these studies has a slight infectivity deficit (≤1 log unit) relative to wild-type *B. burgdorferi* in mice infected by syringe (35), larvae were infected by immersion (49) to ensure that each group contained comparable spirochete loads prior to being fed on a naive mouse. It is important to note that *B. burgdorferi* Δ*hk1* and Δ*rrp1* strains display identical survival defects in larvae infected by the natural and immersion methods and that the survival of both mutants can be restored to wild-type levels by complementation

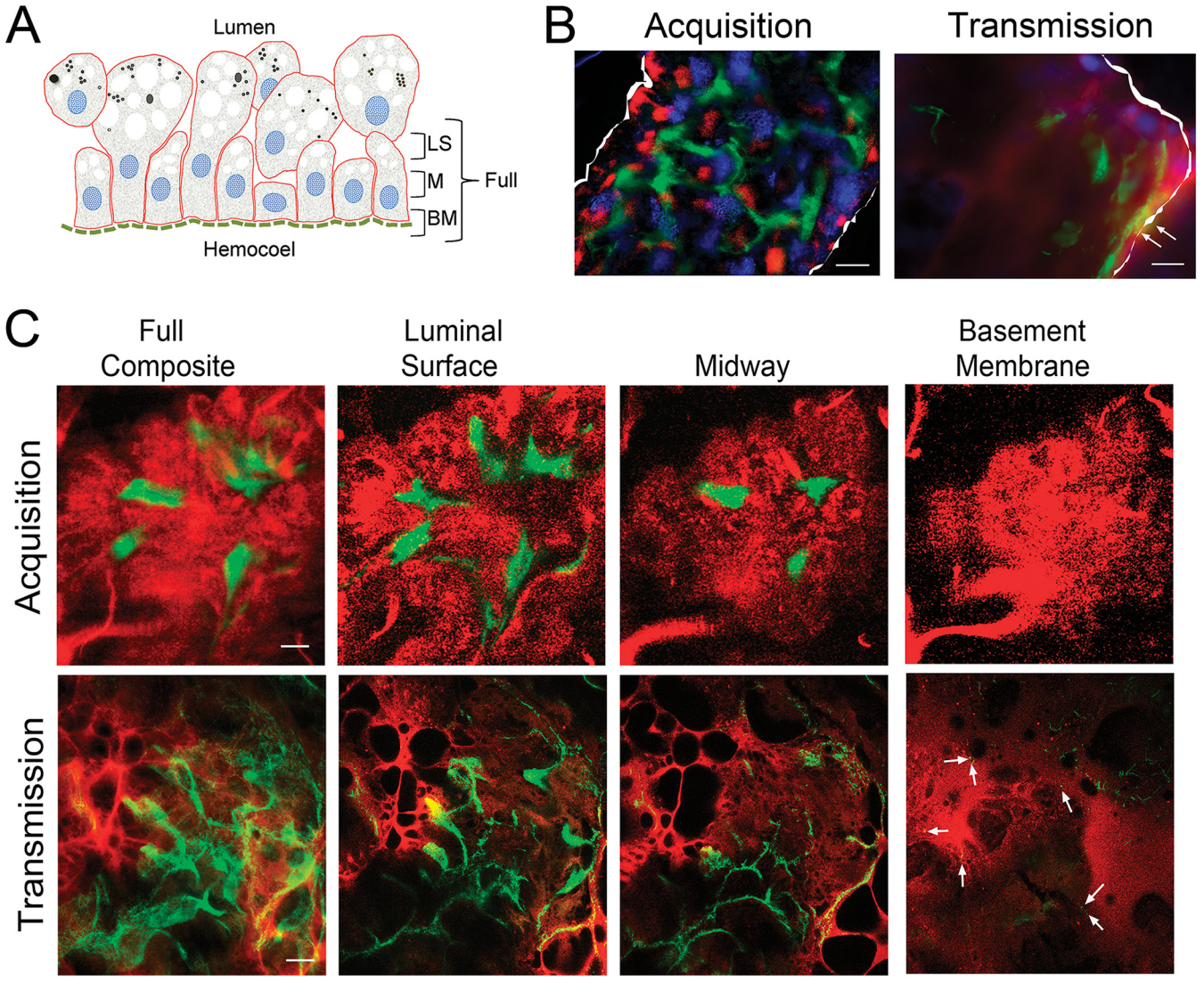

FIG 2 The RpoS-off state during acquisition imparts a Stay signal that promotes midgut colonization without dissemination. (A) Cartoon depicting the midgut epithelium at 72 h postplacement as well as the orientation and location of the confocal optical sections shown in panel C. Abbreviations: LS, luminal surface; M, midway through the epithelium; BM, basement membrane. (B) Representative images of whole-mount intact midguts infected with wild-type *B. burgdorferi* strain 297 expressing GFP (Bb914) examined by epifluorescence microscopy during acquisition and transmission. The panels are color merges of fields containing spirochetes (green), midgut epithelial cells stained with the lipophilic dye FM4-64 (red), and the nuclear dye DAPI (4′,6-diamidino-2-phenylindole) (blue) (6). The perimeters of midguts in the epifluorescence images are outlined in white. Arrows in the transmission epifluorescence image panels indicate networks in close proximity to the basement membrane. (C) Representative Z-series confocal optical sections (1 μm) obtained by imaging of midguts isolated at 72 h postplacement. The leftmost panels depict composite images obtained through the full thickness of the midgut epithelium (basement membrane to luminal surface), while 3-μm composite images are used to show spirochetes at the luminal surface, midway through the epithelium, and at the basement membrane, as depicted in panel A. Arrows in the transmission series indicate spirochetes at the basement membrane. Bars = 25 μm.

(34, 35). Whereas He et al. (35) saw a substantial (10- to 15-fold) decrease in burdens for larvae infected with the Δ*glp* mutant compared to larvae infected with wild-type *B. burgdorferi*, we saw only a modest (~3-fold; $P \leq 0.0001$) difference between these two strains by either qRT-PCR (Fig. 4A) or qPCR (see Fig. S1 in the supplemental material). This difference paled in comparison to the 50- and 180-fold lower burdens in larvae infected with *B. burgdorferi* Δ*hk1* and Δ*rrp1* mutants, respectively (Fig. 4A; see also Fig. S1 in the supplemental material). Furthermore, by immunofluorescence assay, there was no appreciable difference in spirochete burdens in midguts from replete larvae infected with the *B. burgdorferi* wild-type and Δ*glp* isolates, while *B. burgdorferi* Δ*hk1* and Δ*rrp1* isolates were rarely observed (Fig. 4B). Moreover, following the molt, *B. burgdorferi* Δ*glp*-infected nymphs transmitted infection to naive mice, although not quite at wild-type levels, on the basis of culturing of skin from the bite site at the time of repletion and serology and culturing of ear tissue at 4 weeks after the drop-off (Table 1). The relatively small decrease in transmission and infectivity that we observed for the *B. burgdorferi* Δ*glp* mutant is consistent with this strain having only a slight infectivity deficit in mice when it is inoculated by syringe (35). In contrast, none of the mice fed on by *B. burgdorferi* Δ*hk1*- or Δ*rrp1*-infected nymphs seroconverted or were culture positive at the time of repletion (bite site) or 4 weeks after drop-off (ear tissue) (Table 1).

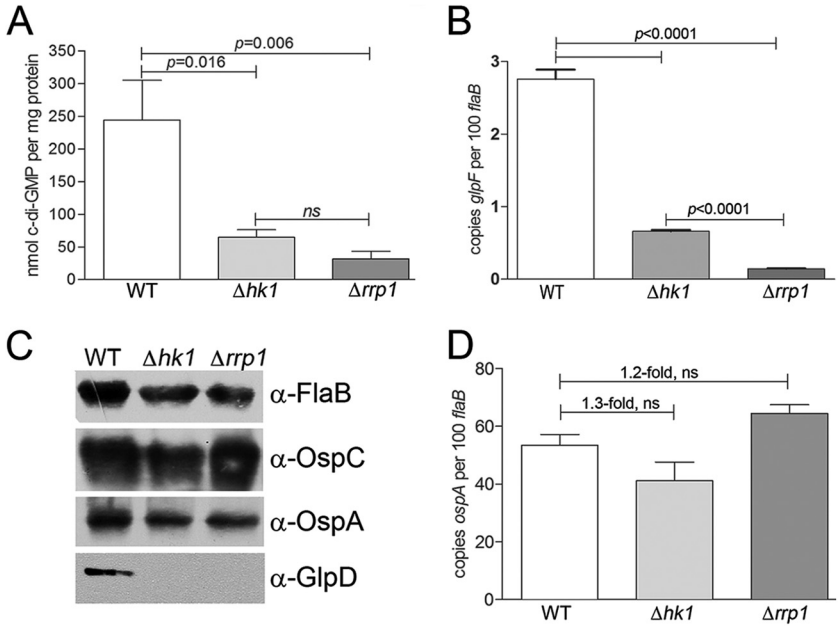

FIG 3 Hk1 and Rrp1 function cooperatively to promote the synthesis of c-di-GMP and expression of c-di-GMP-dependent genes. (A) Intracellular levels of c-di-GMP in whole-cell lysates from *B. burgdorferi* wild-type (Bb1399), Δ*hk1* (Bb1197), and Δ*rrp1* (Bb1451) strains grown *in vitro* following a temperature shift from 23°C to 37°C (three biological replicates per strain), as measured by UPLC/MS/MS (135). The statistical significance of the difference in the results between the wild-type parent and each mutant was determined using an unpaired *t* test. ns, not significant. (B) Transcript levels for *bb0240* (*glpF*) in *B. burgdorferi* wild-type, Δ*hk1*, and Δ*rrp1* strains assayed by qRT-PCR. Values represent the average transcript copy numbers for *bb0240* (*glpF*) ± SEM normalized per 100 copies of *flaB* from at least three biological replicates. Statistical significance was determined by comparing the average normalized copy number values for either mutant with those for the wild-type parent. (C) Whole-cell lysates from *B. burgdorferi* wild-type, Δ*hk1*, and Δ*rrp1* strains grown to late logarithmic phase *in vitro* following a temperature shift from 23°C to 37°C were separated by SDS-PAGE and immunoblotted using antisera against FlaB (loading control), OspC, OspA, and GlpD. (D) Transcript levels for *ospA* in *B. burgdorferi* wild-type, Δ*hk1*, and Δ*rrp1* strains grown to late logarithmic phase *in vitro* following a temperature shift. Values represent the average transcript copy numbers for *ospA* ± SEM normalized per 100 copies of *flaB* from at least three biological replicates.

Defining the Rrp1 regulon *in vitro* by comparative RNA-Seq. The data presented above established that the *B. burgdorferi* Δ*hk1* and Δ*rrp1* mutants have a far more severe survival defect in replete larvae than the *B. burgdorferi* Δ*glp* mutant. Thus, while glycerol uptake and utilization contribute to spirochete survival within the tick, c-di-GMP-regulated genes outside the *glp* operon appear to be required by *B. burgdorferi* to withstand the tick blood meal. We reasoned, therefore, that an understanding of the Δ*hk1* and Δ*rrp1* phenotypes requires an accurate and comprehensive catalog of genes whose expression is modulated by c-di-GMP. Because the *B. burgdorferi* Δ*hk1* and Δ*rrp1* mutants are eliminated from larvae and nymphs at the onset of the blood meal, it is not possible to perform comparative transcriptomics on either mutant in feeding ticks. Instead, we took advantage of the fact that this TCS is active *in vitro*. Two prior studies (35, 43), both of which used microarray analysis to define the Rrp1 regulon, yielded highly discrepant data

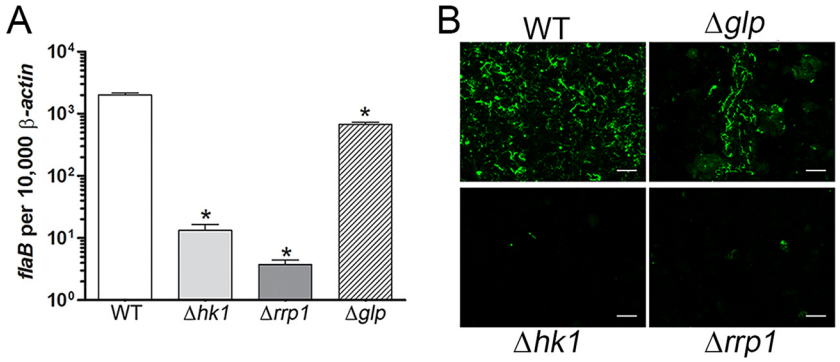

FIG 4 Loss of *glp* gene expression alone cannot account for the survival defect of the *B. burgdorferi* Δ*hk1* and Δ*rrp1* mutants during tick feeding. (A) Burdens were assessed by qRT-PCR using a TaqMan assay for *flaB* and normalized per 1,000 copies of tick β-actin. Bars represent the mean ± SEM for each isolate. Statistical significance was determined by comparing the average value for either mutant to that for its wild-type parent. *, $P \leq 0.0001$. Similar results were obtained by qPCR using DNA extracted from parallel pools of replete larvae (see Fig. S1 in the supplemental material). (B). Representative immunofluorescence images of larvae infected with the designated isolate and fed to repletion on naive C3H/HeJ mice; spirochetes (green) were detected using FITC-conjugated anti-*Borrelia* antibody. Bars = 20 μm.

TABLE 1 *B. burgdorferi* Δ*glp*-infected nymphs transmit infection to naive mice

Strain	Description	No. of bite sites with infected nymphs/no. of bite sites analyzed[a,b]	No. of infected mice/total no. of mice tested 4 wk after drop-off by[b,c]:	
			Serology	Ear biopsy
Bb1399	WT 5A4 NP1 parent	18/18	3/3	3/3
Bb1197	5A4 NP1 Δ*hk1*	0/16[d]	0/3	0/3
Bb1451	5A4 NP1 Δ*rrp1*	0/12	0/3	0/3
Bb1452	5A4 NP1 Δ*glp*	9/18	2/3	2/3

[a] The skin of C3H/HeJ mice (6 sites per mouse) was excised from the site at ~48 to 72 h postrepletion. A minimum of 2 mice were tested per isolate per time point.
[b] Cultures were monitored for spirochetes by dark-field microscopy for at least 4 weeks.
[c] Serology and ear biopsies were performed at 4 weeks postrepletion. Ear tissues were cultured in BSK-II medium containing the appropriate antibiotics.
[d] Two cultures were discarded due to contamination.

TABLE 2 Validation of RNA-Seq data by qRT-PCR

Gene	Fold change in expression between WT and the indicated mutant by[a]:		
	RNA-Seq for Δ*rrp1* mutant	qRT-PCR	
		Δ*rrp1* mutant	Δ*hk1* mutant
ospC (*bbb19*)	1.55	−2.03	−1.01
bb0021	−3.66	−4.47	−1.32
malX-1 (*bb0116*)	−2.27	−6.22	−6.66
glpF (*bb0240*)	11.94	12.77	31.99
glpK (*bb0241*)	10.70	12.97	11.68
glpD (*bb0243*)	12.30	11.37	26.62
bb0323	2.33	1.88	2.47
bb0629	2.21	6.69	−1.05
bosR (*bb0647*)	1.56	1.41	1.23
bb0680	2.14	5.29	1.15
rpoS (*bb0771*)	3.35	1.64	−1.14
spoVG (*bb0785*)	3.00	3.05	6.30
arcA (*bb0841*)	2.40	1.11	−1.58
bba07	3.60	2.84	2.45
ospA (*bba15*)	1.05	−1.20	−1.30
dbpA (*bba24*)	−1.07	−1.83	−1.40
bba52	2.81	3.80	5.53
bba57	2.68	1.65	4.13
bba59	2.10	3.69	6.00
lp6.6 (*bba62*)	2.31	2.67	1.98
bba73	2.60	2.05	1.95
bba74	7.51	6.12	12.36
malX-2 (*bbb29*)	2.19	6.01	10.84
bbh28	2.79	6.97	6.92
bbo39	3.44	3.44	−1.30
bbp38	3.76	3.47	1.50
bbq47	2.60	2.67	−3.22
ospE	3.02	3.23	1.89

[a] See Fig. S3 in the supplemental material for a graphical display of these data.

sets. Consequently, we undertook our own reassessment of the Rrp1 regulon using RNA-Seq, which provides an unbiased survey of transcripts over an extremely broad, dynamic range (75, 76). Prior to generating Illumina TruSeq libraries, we confirmed that all three biological replicates of the wild-type parent (Bb1286) expressed highly similar levels of Rrp1 and the Rrp1-dependent gene product BB0243/GlpD (see Fig. S2 in the supplemental material); as expected, neither protein was detected in the Δ*rrp1* mutant (strain Bb1520). At the outset, we validated our RNA-Seq data (presented in their entirety in Table S2 in the supplemental material) by performing qRT-PCR on a diverse panel of 28 genes using RNAs extracted from *B. burgdorferi* wild-type and Δ*rrp1* isolates cultivated *in vitro* following a temperature shift. In almost all cases, the differences in transcript levels between the *B. burgdorferi* Δ*rrp1* and wild-type isolates were comparable ($R^2 = 0.7904$) to those observed by RNA-Seq (Table 2; see also Fig. S3 in the supplemental material). With only a few exceptions, the expression profiles of the Δ*hk1* and Δ*rrp1* mutants were highly similar (Table 2; see also Fig. S3 in the supplemental material), providing further evidence that Hk1 is the cognate sensor kinase for Rrp1.

The Rrp1 regulon contained 219 differentially expressed genes (see Table S2 in the supplemental material): 161 expressed at higher levels (i.e., upregulated by c-di-GMP) and 58 expressed at lower levels (i.e., downregulated by c-di-GMP) in the wild type than in *B. burgdorferi* Δ*rrp1*. Of the two prior microarray analyses (35, 43), our RNA-Seq data aligned most closely with those of He et al. (35) (~35% concordance, compared to a 20% concordance with the RNA-Seq data of Rogers et al. [43]). The low concordance between data sets likely reflects differences in the isolates (5A4 NP1 versus A3) and methodology (RNA-Seq versus microarray analysis) used in each study. However, all three studies are in agreement regarding a role for c-di-GMP in modulating the expression of the *glp* operon, the OspE, OspF, Elp, and Mlp lipoproteins encoded on the cp32 plasmids, and inner membrane (IM)-associated Bdr paralogs (see below).

Cell envelope-associated gene products. Remarkably, 85 of the 219 genes differentially regulated by c-di-GMP encode proteins that are known or predicted to be associated with the spirochetal cell envelope (Table 3).

(i) Lipoproteins. c-di-GMP upregulated the expression of multiple lipoproteins belonging to the *ospE*, *ospF*, *elp*, and *mlp* families (1). Importantly, RNA-Seq, unlike 70-mer glass slide microarrays, enabled us to unambiguously distinguish between closely related paralogs within each lipoprotein family (77–79). Members of the OspE family, also referred to as BbCrasps, have been shown to inhibit complement-mediated lysis by binding complement factor H (CFH) and CFH-related proteins (1, 80, 81), while the functions of the OspF, Elp, and Mlp families remain to be determined. *bb0323* encodes an OM-associated lipoprotein that interacts with peptidoglycan via a C-terminal LysM domain and is well expressed in feeding larvae and nymphs (82). BB0323-deficient *B. burgdorferi* isolates display an aberrant OM organization and cell division *in vitro* and reduced infectivity in mice and do not survive the blood meal or get transmitted by nymphs (82, 83). *bba62* encodes Lp6.6, an OM-associated lipoprotein that appears to be required throughout the tick phase of the enzootic cycle (32, 84). *B. burgdorferi*, an absolute amino acid auxotroph, acquires amino acids and oligopeptides from the host via an ABC transporter oligopeptide permease (Opp) system (15, 85). Interestingly, two of *B. burgdorferi*'s five OppA substrate-binding lipoproteins (encoded by *bbb16* [*oppA*IV] and *bba34* [*oppA*V]) were differentially regulated by c-di-GMP but in an opposing manner: *oppA*IV was upregulated, while *oppA*V, the only RpoS-dependent *oppA* paralog (24, 86), was downregulated. Only two other lipoproteins (encoded by *bb0298* and *bb0542*) were downregulated by c-di-GMP. Both of these contain tetratricopeptide repeats (TPRs),

TABLE 3 Cell envelope-associated genes regulated by c-di-GMP

Protein and gene	Symbol	Description[a]	Fold change in regulation[b] (WT/Δ*rrp1*)
Putative/known lipoproteins			
bba32		Hypothetical protein	NE
bba60		Surface lipoprotein P27	10.14
bbm28	*mlpF*	MlpF	7.63
bbq35	*mlpJ*	MlpJ	6.91
bbs30	*mlpC*	MlpC	6.59
bbo39	*erpL*	ErpL	6.05
bbq03		Lipoprotein	6.04
bbp28	*mlpA*	MlpA	5.99
bbb27		Hypothetical protein	5.89
bbo28	*mlpG*	MlpG	5.52
bbs41	*erpG*	ErpG	5.12
bbb08		Hypothetical protein	4.58
bbl40	*erpO*	ErpO	4.52
bbl28	*mlpH*	MlpH	4.30
bbi16		Hypothetical protein	4.01
bbm27	*revA*	Rev protein	3.96
bbo40	*erpM*	ErpM	3.94
bbp39	*erpB*	ErpB	3.90
bbn28	*mlpI*	MlpI	3.85
bbp38	*erpA*	ErpA	3.76
bbl39	*erpN*	ErpN	3.14
bbn38	*erpP*	ErpP	3.02
bbn39	*erpQ*	ErpQ	2.99
bbk48		Immunogenic protein P37	2.94
bba04		S2 antigen	2.94
bba07	*chpA1*	ChpA1 protein	2.93
bbb16	*oppA*IV	ABC-type oligopeptide transport (Opp) system periplasmic solute-binding protein component OppAIV	2.80
bba05		S1 antigen	2.77
bba57		Lipoprotein	2.68
bbb09		Hypothetical protein	2.65
bba73		P35 antigen, putative	2.60
bbq47	*erpX*	ErpX	2.60
bba69		Hypothetical protein	2.57
bbe31		P35 antigen, putative	2.53
bba66		Lipoprotein	2.46
bbr42	*erpY*	ErpY	2.45
bbi42		Hypothetical protein	2.41
bb0323		LysM domain-containing protein	2.33
bba62	*lp6.6*	Lipoprotein	2.31
bbk49		Hypothetical protein	2.30
bbr28	*mlpD*	MlpD	2.23
bbp27	*revA*	Rev protein	2.23
bbk50		P37 immunogenic protein	2.14
bba59		Lipoprotein	2.10
bba65		Lipoprotein	2.09
bb0689		Hypothetical protein	2.09
bba34	*oppA*V	ABC-type oligopeptide transport system (Opp) periplasmic solute-binding protein protein component OppAV	−2.29
bb0298		TPR domain-containing protein	−2.08
bb0542		TPR domain-containing protein	−2.03
Inner membrane-associated proteins			
bb0240	*glpF*	Glycerol uptake facilitator	11.94
bbq34	*bdrW*	BdrW	6.66
bbs29	*bdrF*	BdrF	3.46
bbn27	*bdrR*	BdrR	3.38
bbb04	*chbB*	PTS system, chitobiose-specific EIIC component	3.10
bbb03	*resT*	Telomere resolvase	3.01
bbl35	*bdrO*	BdrO	2.61

(Continued on following page)

TABLE 3 (Continued)

Protein and gene	Symbol	Description[a]	Fold change in regulation[b] (WT/Δ*rrp1*)
bb0409		Hypothetical protein	2.58
bb0591		Competence locus E, putative	2.56
bbp34	*bdrA*	BdrA	2.43
bb0631		Hypothetical protein	2.31
bbq42	*bdrV*	BdrV	2.23
bbs37	*bdrE*	BdrE	2.22
bb0629	*fruA-2*	PTS system, mannose-specific EIIABC component	2.21
bbb29	*malX-2*	PTS system, GlcNAc/glucose-specific EIIABC component	2.19
bbi38		Hypothetical protein	2.07
bbh13		Hypothetical protein	2.04
bbj41		P35 antigen, putative	2.02
bb0373		Hypothetical protein	−6.37
bb0580		Conserved hypothetical integral membrane protein	−6.13
bb0694	*ffh*	Signal recognition particle protein	−3.44
bb0397		Putative inner membrane protein	−2.90
bb0442		Putative membrane protein insertase	−2.40
bb0146	*proV*	Glycine betaine, L-proline ABC transporter, ATP-binding protein	−2.36
bb0116	*malX-1*	PTS system, GlcNAc/glucose-specific EIIABC component	−2.27
bb0754		ABC transporter, ATP-binding protein	−2.13
bb0170		Hypothetical protein	−2.07
bb0089		Hypothetical protein	−2.04
Putative outer membrane-spanning and periplasmic proteins			
bba74	*bba74*	Outer membrane-associated periplasmic protein	7.51
bbi31		P13 porin paralog	5.21
bbq06		P13 porin paralog	4.33
bbh41		P13 porin paralog	3.77
bba52		Putative periplasmic protein	2.81
bb0418	*dipA*	Dicarboxylate-specific porin A	2.47
bb0624		Hypothetical protein	−2.25
bb0794		Hypothetical protein	−2.06

[a] Annotations and gene product descriptions are based on those provided by the Spirochetes Genome Browser (sgb.fli-leibniz.de).
[b] Fold regulation based on RNA-Seq. See Table S2 in the supplemental material for the complete data set. NE, not expressed by the *B. burgdorferi* Δ*rrp1* mutant.

ubiquitous structural motifs thought to mediate protein-protein interactions (87).

(ii) IM-associated proteins. Eighteen gene products upregulated by c-di-GMP, including 7 *Borrelia* direct repeat (Bdr) proteins (88–90), are predicted to localize to the spirochete's IM. While the function(s) of the Bdr paralogs has yet to be determined, the presence of a putative serine-threonine phosphorylation domain led Marconi and colleagues (88, 89) to suggest that they play a possible role in cell signaling. The downregulation of *bb0146* (*proV*), encoding the ATPase component of a glycine betaine, L-proline ABC transporter, is particularly noteworthy. Glycine betaine, an osmoprotectant (91), has been shown to negatively affect bacterial growth under conditions when ATP is limiting (91), as is likely the case for *B. burgdorferi* in the tick midgut.

(iii) Outer membrane-spanning and periplasmic proteins. At least four genes upregulated by c-di-GMP encode known or putative porins: DipA (encoded by *bb0418*) (92) and the three P13 paralogs (encoded by *bbh41*, *bbi31*, and *bbq06*) (93). P13 paralogs are thought to function as general diffusion porins, while DipA has a high affinity for dicarboxylates, including glutamate and pyruvate (92), which may help protect *B. burgdorferi* against oxidative damage within the fed midgut milieu. On the basis of bioinformatics analyses (see Materials and Methods), two additional genes (*bb0624* and *bb0794*) upregulated by c-di-GMP are predicted to encode OM-spanning (i.e., β-barrel) proteins. *bba74*, formerly *oms28*, encodes a periplasmic protein of unknown function that is expressed exclusively during tick feeding and repressed by RpoS within the mammal (38, 94).

Metabolism and physiology. c-di-GMP upregulated the expression of *bb0622* (*ackA*), the acetate kinase required to generate acetyl phosphate (acetyl-P), the high-energy phosphate donor responsible for activation of the RpoS pathway via Rrp2 (18). Acetyl-P also serves as the substrate for phosphate acetyltransferase (Pta), which gives rise to acetyl coenzyme A (acetyl-CoA), an important intermediary metabolite for cell wall synthesis via the mevalonate pathway (18, 95). Interestingly, two genes, *bb0683* and *bb0685*, encoding 3-hydroxyl-3 methylglutaryl (HMG)-CoA synthase and reductase, the enzymes responsible for the second and third steps within the mevalonate pathway, respectively (95), were downregulated by c-di-GMP. Recently, we reported that genes within the mevalonate pathway are expressed at higher levels in dialysis membrane chambers (DMCs) than in fed nymphs (42), a finding that is consistent with their expression being suppressed by c-di-GMP. Five genes encoding phosphotransferase system (PTS) sugar transporter (EII) components for mannose (*bb0629*), chitobiose (*bbb04* to *bbb06*), and GlcNAc (*bbb29* [*malX-2*])

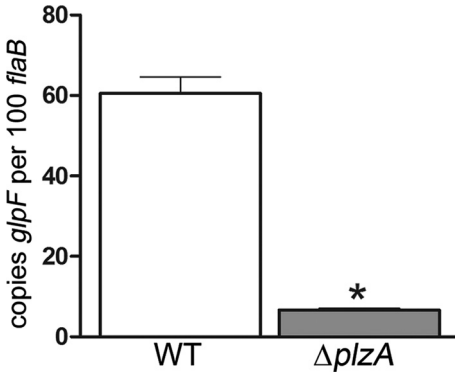

FIG 5 The c-di-GMP effector protein PlzA is required for expression of the *glp* operon. Transcript levels for *bb0240* (*glpF*) in a wild-type (WT) *B. burgdorferi* strain (Bb1286) and the *B. burgdorferi* Δ*plzA* isolate (Bb1548) grown to late logarithmic phase following a temperature shift *in vitro*. Values represent the average transcript copy numbers for *glpF* ± SEM normalized per 100 copies of *flaB*. *, $P \leq 0.0001$.

(14, 96) were upregulated by c-di-GMP, while *bb0116* (*malX-1*), encoding a second putative GlcNAc transporter (14), was downregulated. *B. burgdorferi* also expressed higher levels of amylomaltase (*bb0166* [*malQ*]) in response to c-di-GMP; however, this gene is not required by *B. burgdorferi* to complete its enzootic cycle (97). Lastly, we saw increased expression of *bb0084*, encoding a putative SufS-like cysteine desulfurase involved in Fe-S cluster biosynthesis (98), in response to c-di-GMP. Increased levels of BB0084 may enhance redox sensing by *B. burgdorferi* and/or counteract redox-related stress during tick feeding (99). The presence of this enzyme argues, contrary to the report by Posey and Gherardini (100), that *B. burgdorferi* contains iron; of note, Wang et al. (101) recently confirmed, using high-resolution mass spectrometry, iron uptake by *B. burgdorferi*.

Gene regulation. Little is known about the mechanism(s) by which c-di-GMP modulates gene expression in *B. burgdorferi*. To date, only one c-di-GMP-binding protein, BB0733/PlzA, has been identified in *B. burgdorferi* (102, 103). Because PlzA lacks a readily identifiable DNA-binding domain, it is presumed to act via an as yet unknown partner. The *B. burgdorferi* Δ*plzA* mutant was found by qRT-PCR to express significantly lower levels of *bb0240* (*glpF*) *in vitro* than the wild-type parent (Fig. 5), thereby confirming a role for this novel effector protein in modulating transcription in *B. burgdorferi*. Interestingly, expression of *plzA* was downregulated by c-di-GMP, suggesting the existence of a regulatory circuit in which high levels of c-di-GMP promote the allosteric activation of PlzA (and increased expression of PlzA-dependent genes), while at the same time negatively regulating the expression of *plzA*. The *B. burgdorferi* genome encodes only a small number of putative *trans*-acting factors. Two of these (*bb0785* [*spoVG*] and *bb0693* [*badR*]) were differentially regulated by c-di-GMP. *bb0785*, which was upregulated by c-di-GMP, encodes the recently described DNA-binding protein SpoVG (104). The promoter targets for SpoVG have yet to be defined. *bb0693*, encoding the carbohydrate-responsive repressor protein BadR (105), was downregulated by c-di-GMP. BadR has been linked to repression of the chitobiose transporter genes (*bbb04* to *bbb06*) (105); thus, it is possible that the increased expression of chitobiose genes in the wild type compared to that in *B. burgdorferi* Δ*rrp1* is due to the loss of BadR-mediated repression.

Expression of Hk1/Rrp1-regulated genes by wild-type *B. burgdorferi* is enhanced in feeding ticks compared to mammals. The dramatic survival defect of the *B. burgdorferi* Δ*hk1* and Δ*rrp1* mutants in ticks led us to hypothesize that the Hk1/Rrp1 TCS controls the expression of genes required to counter noxious substances encountered within the midgut during the blood meal (34). As noted above, it is not possible to perform comparative transcriptomics on either mutant in feeding ticks. Thus, to better understand when during the enzootic cycle these genes function, we performed qRT-PCR on a broad panel of c-di-GMP-upregulated genes identified by RNA-Seq using RNAs isolated from wild-type strain 5A4 NP1 (Bb1286) within replete larvae, engorged nymphs, and DMCs. As shown in Fig. 6A to C, all 18 c-di-GMP-upregulated genes examined were expressed at significantly higher levels in fed larvae and/or nymphs than in DMCs. Five of the c-di-GMP-upregulated genes examined (Fig. 6B) are repressed by RpoS within the mammal (19, 24, 46), and as such, their decreased expression in DMCs is likely due to a combination of decreased c-di-GMP- and RpoS-mediated repression. Interestingly, we detected higher transcript levels for all 18 c-di-GMP-upregulated genes in transmitting nymphs than acquiring larvae (Fig. 6A and B), a surprising dichotomy, given that the pronounced survival defects of the *B. burgdorferi* Δ*hk1* and Δ*rrp1* mutants in these two tick life stages are indistinguishable (34, 35). Presumably, increased expression of these genes reflects the presence of higher levels of c-di-GMP.

c-di-GMP enhances expression of select RpoS-dependent genes during transmission. Lastly, we sought to gain additional insight into whether c-di-GMP modulates RpoS-dependent gene expression during the enzootic cycle. We began by comparing the Rrp1 regulon, defined herein by RNA-Seq, with the RpoS regulon, defined previously by microarray using strain 297 Δ*rpoS* (24), to determine the extent to which the Rrp1 and RpoS regulons overlap. This comparison yielded 41 c-di-GMP-upregulated genes whose expression requires RpoS (see Table S2 in the supplemental material). Because the RpoS regulon for the B31 strain (5A4 NP1) used herein has not been defined, we used published microarray data (106) for a B31 5A4 NP1 Δ*rrp2* mutant to identify RpoS-dependent genes common to both B31 and 297; of note, Rrp2 is absolutely required for RpoN-mediated transcription of *rpoS* in *B. burgdorferi* (107). Of the 24 c-di-GMP-upregulated genes that appear to be transcribed by RpoS in both 297 and B31 (see Table S2 in the supplemental material), three (*bb0680*, *bba07*, and *bba73*) were selected for expression profiling analysis by qRT-PCR in replete larvae, engorged nymphs, and DMCs. As shown in Fig. 6C, none was expressed in fed larvae, a result entirely consistent with *B. burgdorferi* being in an RpoS-off state during acquisition (Fig. 1B). On the other hand, all three RpoS-dependent genes were expressed by *B. burgdorferi* in engorged nymphs and DMCs (Fig. 6C), the two stages in which RpoS is in the on state (1, 17). Surprisingly, we saw significantly higher transcript levels for all three genes in nymphs compared to DMCs (Fig. 6C). This finding prompted us to assess transcript levels for *ospC* and *dbpA*, two RpoS-dependent genes that function exclusively within the mammal (19, 66, 108–112) and whose expression is unaffected by c-di-GMP (see Fig. S3 in the supplemental material). As shown in Fig. 6D, *ospC* and *dbpA* were expressed at similar or significantly higher levels in DMCs, respectively, compared with their levels of expression in nymphs.

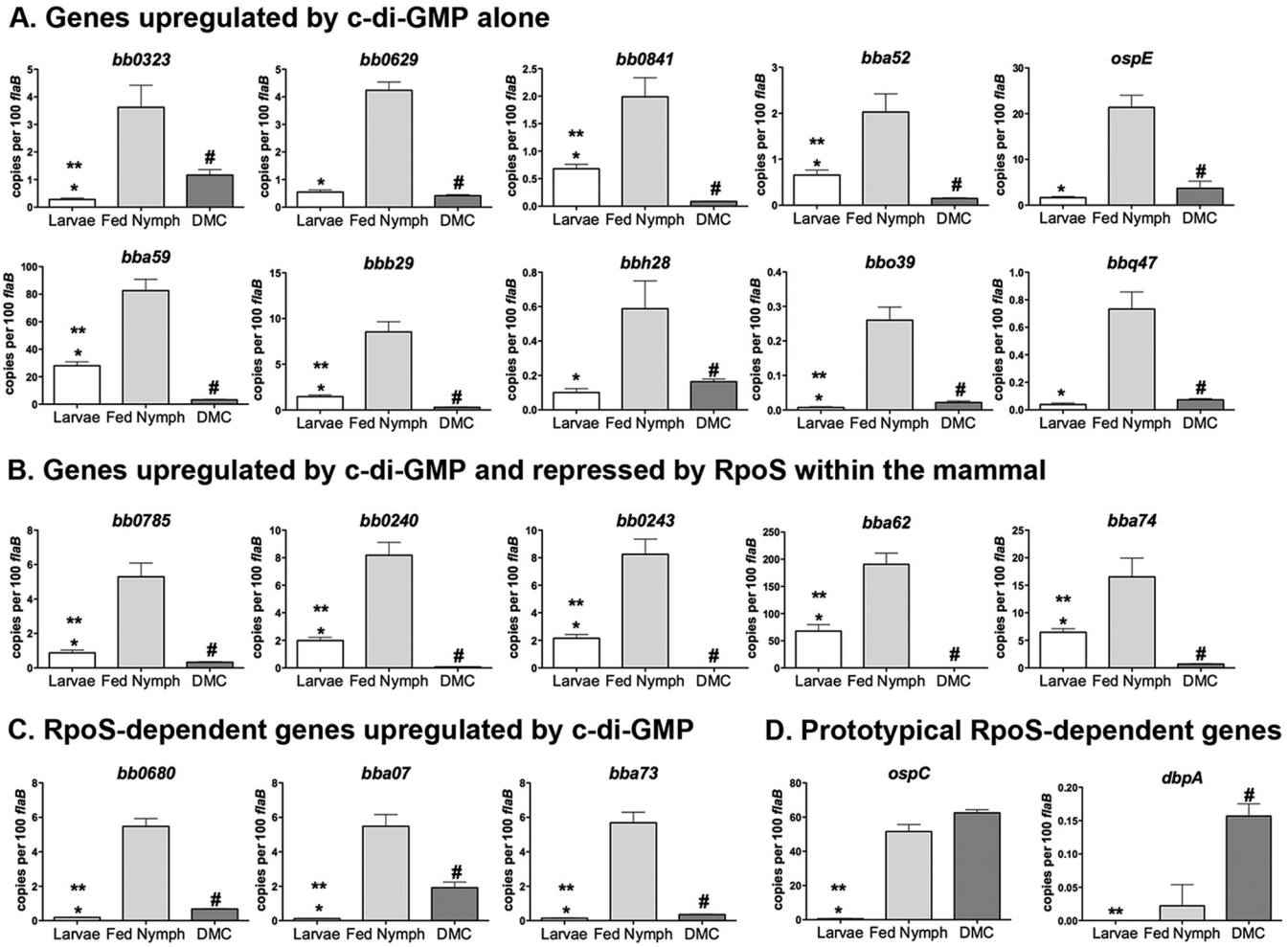

FIG 6 Contours of c-di-GMP-mediated gene regulation throughout the enzootic cycle. qRT-PCR of genes that are upregulated by c-di-GMP alone (A), upregulated by c-di-GMP but repressed by RpoS within the mammal (B), and transcribed by RpoS and upregulated by c-di-GMP (C) and of prototypical RpoS-dependent genes that function within the mammal (D) was performed. cDNAs were generated from *B. burgdorferi* strain B31 5A4 NP1 (Bb1286) obtained from replete larvae (Larvae), from engorged nymphs (Fed Nymph), and following cultivation within DMCs. Values represent the average transcript copy number ± SEM normalized per 100 copies of *flaB*. *P* was ≤0.03 for larvae versus nymphs (*), larvae versus DMCs (**), and nymphs versus DMCs (#). RpoS dependence is based on previously published results of microarray analyses comparing wild-type and RpoS-deficient strain 297 isolates (24) and comparing wild-type and Rrp2-deficient strain 5A4 NP1 isolates (106).

DISCUSSION

Tick feeding provides Lyme disease spirochetes with the windows of opportunity needed to transit between their mammalian reservoir host(s) and arthropod vector. During the acquisition and transmission blood meals, *B. burgdorferi*, an extreme auxotroph, must adapt physiologically to the fed midgut milieu, particularly with respect to the use of alternate carbon sources (12–14). Spirochetes also must cross physical barriers (i.e., peritrophic and basement membranes) and evade the tick's innate immune defenses, which includes antimicrobial peptides and defensins, lysozyme, agglutinins/lectins, complement-related molecules, and reactive oxygen species (ROS) (4, 7–11). In order to migrate into and out of the vector, *Borrelia* must sense and respond to chemotactic signals encountered within the bite site and midgut, respectively (113, 114). Two regulatory systems, the Hk1/Rrp1 TCS and the Rrp2/RpoN/RpoS pathway, are essential for orchestrating the expression of the gene products that *B. burgdorferi* requires to meet the demands of its enzootic cycle (1, 17). The studies presented herein were undertaken to further our understanding of how these genetic programs promote *B. burgdorferi*'s unique dual host lifestyle. First, we sought to clarify how the RpoS-off state influences spirochete behavior during acquisition, when the Hk1/Rrp1 TCS is first activated. We next undertook a careful reassessment of the Rrp1 regulon by RNA-Seq to better ascertain how c-di-GMP promotes spirochete survival within feeding ticks. Lastly, we used qRT-PCR to examine the expression profiles of c-di-GMP-regulated genes through the enzootic cycle. Results from these studies add to a growing body of evidence for the regulatory interplay between c-di-GMP and RpoS (115, 116).

Our previous designation of RpoS as the gatekeeper was based on our finding that the absence of RpoS during acquisition allows the derepression of tick-phase genes (19, 24, 46). In the present study, confocal imaging revealed that wild-type spirochetes within acquiring nymphs did not form adherent networks or penetrate the midgut epithelium, two hallmarks of transmission (6, 19). By qRT-PCR, we established that spirochetes within acquiring nymphs, like those in

larvae, are in an RpoS-off state. Together, these data have enabled us to extend our conceptualization of RpoS's gatekeeper function. At the onset of transmission, the synthesis of RpoS induces the tightly coordinated expression of genes required for physiological adaptation to the blood meal (i.e., *cdr*) (117), network formation (*i.e.*, *bba64*) (118, 119), chemotactic migration out of the midgut (i.e., *mcp-4* and *mcp-5*), and early mammalian infection (i.e., *ospC* and *dbpBA*) (19, 66, 108). Collectively, we liken the RpoS-on state to a Go signal for tick-to-mammal transmission (19). The RpoS-off state, on the other hand, appears to confer a stay signal that promotes relatively superficial interactions between *B. burgdorferi* and the tick midgut epithelium. Recent microarray analyses of *B. burgdorferi* within fed larvae and nymphs suggest that, like the Go signal, the Stay signal involves a multitude of genes products involved in *B. burgdorferi*-tick surface interactions and metabolic adaption to the fed midgut (42). Our ability to use nymphs as larval surrogates clearly demonstrates that the transcriptional changes and migratory behavior associated with acquisition are driven by the receptiveness of spirochetes to exogenous signals encountered within the bite site rather than the tick life stage.

In addition to the behavioral changes brought on by the Stay signal, acquisition requires activation of the Hk1/Rrp1-mediated survival program. He et al. (35) attributed the killing of the *B. burgdorferi* Δ*rrp1* mutant in feeding ticks primarily to a metabolic deficit brought on by the inability to use glycerol as a carbon/energy source. In our side-by-side comparisons, however, we saw a marked difference in the survival and transmissibility between the *B. burgdorferi* Δ*glp* mutant and the *B. burgdorferi* Δ*hk1* and Δ*rrp1* mutants. Contrary to the findings of He et al. (35), we saw only a modest decrease in the survival of the *B. burgdorferi* Δ*glp* mutant in replete larvae, and following the molt, *B. burgdorferi* Δ*glp*-infected nymphs transmitted infection to mice. Virtually no *B. burgdorferi* Δ*hk1* and Δ*rrp1* mutant spirochetes survived the larval blood meals, and none of the mice fed on by *B. burgdorferi* Δ*hk1*- or Δ*rrp1*-infected nymphs seroconverted. The ability of the Δ*glp* mutant to persist through the molt likely stems from the fact that *B. burgdorferi* can generate glycerol-3-phosphate from an alternative pathway involving BB0368/GpsA, an *sn*-glycerol-3-dehydrogenase, and the glycolytic intermediate dihydroxyacetone phosphate (12, 15). Collectively, our data demonstrate convincingly that the protective effect of c-di-GMP extends beyond glycerol utilization.

The borrelial OM is extremely fragile and easily disrupted by physical manipulation and/or chemical agents, such as detergents (120). Membrane lipids are also the primary target for ROS in *B. burgdorferi* (7); oxidation of membrane lipids decreases membrane fluidity and can lead to the formation of membrane blebs, while lipid peroxides and their degradative products (e.g., aldehydes) can damage membrane-associated proteins, such as solute transporters (7). During tick feeding, spirochetes encounter an array of noxious substances, including salivary and midgut digestive and host/tick innate immune defenses, such as complement, antimicrobial peptides, and ROS (4, 7–11). Thus, one possible explanation for the survival defect of the *B. burgdorferi* Δ*hk1* and Δ*rrp1* mutants is that they are unable to fortify their cell envelopes against these exogenous stressors. The Hk1/Rrp1 TCS, either directly or indirectly, upregulates the expression of ~160 genes, nearly half of which encode gene products associated with the cell envelope. A substantial proportion of these c-di-GMP-upregulated genes encode lipoproteins, including members of the OspE, OspF, and Mlp families (1). The OspE paralogs are particularly noteworthy, given the function of these lipoproteins in protecting against complement (80). One can easily envision the *glp* gene products being part of this scenario, given that glycerol-3-phosphate is required for synthesis of the phospholipid precursor phosphatidic acid (121), in addition to being an alternate carbon source (12). It is worth noting that links between TCS and remodeling of the bacterial cell envelope in stressful milieus are well documented, with Cpx in *E. coli*, PhoPQ in *Salmonella enterica* serovar Typhimurium, and MprAB in *Mycobacterium tuberculosis* being among the best-characterized examples (122–128).

Our genome-wide transcriptomic analyses also provided insight into additional mechanisms whereby c-di-GMP-regulated gene products could function, in addition to or alongside cell envelope remodeling, to promote survival within the fed tick milieu. *B. burgdorferi*, an extreme autotroph, must acquire metabolites and biochemical intermediates from the host (15). One important component of *B. burgdorferi*'s pathogenic strategy, therefore, is the ability to take advantage of alternate carbon and energy sources throughout its enzootic cycle (12, 14, 15, 85, 96, 97). In addition to the *glp* operon, c-di-GMP induced the expression of general and specific porins, an oligopeptide substrate-binding protein (OppAIV), and PTS sugar transporters specific for chitobiose and GlcNAc. These data raise the possibility that metabolic factors could be contributing, either directly or indirectly, to the decreased survival of the *B. burgdorferi* Δ*hk1* and Δ*rrp1* mutants in ticks. Interestingly, many of the nutrients taken up by these c-di-GMP-regulated gene products are involved in both intermediary metabolism and cell wall biosynthesis. c-di-GMP also upregulated *ackA*, encoding an acetyl phosphate kinase, which is required for the synthesis of acetyl-CoA, an intermediary metabolite involved in cell wall biosynthesis via the mevalonate pathway. In other bacteria, c-di-GMP is associated with the transition between motile and sessile states (129). By RNA-Seq, two chemotaxis-related genes, *mcp-4* and *mcp-5*, were upregulated by c-di-GMP, while two others, *mcp-1* and *cheA2*, were downregulated. Consistent with this finding, Rrp1-deficient *B. burgdorferi* displayed reduced chemotaxis *in vitro* (36, 103). Sultan et al. (130) recently reported that *B. burgdorferi* Δ*motB* mutants, which retained their normal flat-wave morphology but were unable to rotate their flagella, showed decreased survival in feeding nymphs and did not get transmitted to mice via tick bite (130). Thus, *B. burgdorferi* Δ*hk1* and Δ*rrp1* mutants may be unable to migrate to protective niches within the midgut, such as the endoperitrophic space. Lastly, c-di-GMP is known to exert its effector function by diverse mechanisms, including posttranscriptional and posttranslational regulation, riboswitches, and allosteric controls (129). Thus, it is possible that the survival response mediated by c-di-GMP in *B. burgdorferi* involves additional as yet unidentified borrelial constituents and signaling pathways.

Given that the Hk1/Rrp1 TCS is required during both acquisition and transmission, we were surprised to see that all of the c-di-GMP genes examined by qRT-PCR were expressed at significantly higher levels in fed nymphs than in larvae. Presumably, increased expression of these genes reflects the presence of higher levels of c-di-GMP within feeding nymphs. One implication of these data is that spirochetes perceive the larval and nymphal environments differently. Our recent structural analysis of the Hk1 sensor (131) provides insight into how *B. burgdorferi* might regulate and/or fine-tune c-di-GMP synthesis in these two environments. Signal perception by the Hk1/Rrp1 TCS is mediated by

Hk1's periplasmic sensor, which is comprised of three distinct periplasmic substrate-binding protein (PBP) domains (34). Ligand binding by sensor PBPs is thought to induce a conformational change (e.g., from open to closed) within the histidine kinase sensor which, when transmitted across the IM, activates the histidine kinase core (132–134). Nonsynonymous amino acid differences between the putative ligand binding pockets for Hk1's three sensor PBP domains suggest that each binds a different ligand (131). Thus, we envision at least two possible explanations for the increased expression of c-di-GMP-regulated genes in larvae versus nymphs. First, it is possible that the ligand(s) responsible for activating Hk1 is present in higher concentrations in nymphs than in larvae. Alternatively, maximal activation of Hk1 may require a specific combination of host- and/or tick-derived ligands that is present only during the transmission blood meal. Of course, these two possibilities are not mutually exclusive. The increased expression of c-di-GMP-regulated genes in nymphs compared to larvae may reflect the need for enhanced protection within the midgut of the more developed nymphal life stage.

Lastly, the studies presented herein provide provocative new insight into how the Hk1/Rrp1 TCS and RpoS pathways interface throughout *B. burgdorferi*'s enzootic life cycle. Using microarray-based transcriptomics analyses of spirochetes within feeding ticks and DMCs, we recently found that, rather than being induced *en masse*, RpoS-mediated transcription of individual genes is subject to hierarchical control mechanisms that are fine-tuned as transmission progresses and spirochetes establish themselves within the mammal (42). By comparing the RpoS and Rrp1 regulons defined by microarray analysis and RNA-Seq, respectively, we identified a group of genes that appear to be transcribed by RpoS and upregulated by c-di-GMP. The expression profiles of these genes in fed nymphs and DMCs were strikingly different from those of *ospC* and *dbpA*, two RpoS-dependent genes that are induced during transmission but function within the mammal (19, 66, 108–112). Taken together, these data lead us to hypothesize that c-di-GMP selectively enhances the transcription of RpoS-dependent genes that promote tick-to-mammal transmission. As part of its gatekeeper function, RpoS also represses the expression of σ^{70}-dependent tick-phase genes, including *ospA*, *bba62*, and the *glp* operon, within the mammal. Although RpoS-mediated repression of these tick-phase genes begins during the transmission blood meal, it is not complete until *B. burgdorferi* becomes fully adapted to the mammalian host (19). Whereas we formerly attributed this delayed repression to a requirement for additional mammalian host-specific signals (24, 46), our finding that *bba62* and the *glp* operon are upregulated in the wild-type parent compared to the Δ*rrp1* mutant raises the possibility that c-di-GMP antagonizes RpoS-mediated repression within feeding ticks, perhaps by acting allosterically on an RpoS-dependent repressor. Once *B. burgdorferi* is in the mammal, decreased levels of c-di-GMP would allow unfettered repression of these tick-phase genes. Paradoxically, the absence of c-di-GMP cannot explain the RpoS-mediated repression of *ospA* in the mammal because, as shown herein, this gene is not part of the Rrp1 regulon.

ACKNOWLEDGMENTS

This work was supported by Public Health Service grants AI-29735 (to J.D.R. and M.J.C.), AI-85248 (to M.J.C.), and GM103447 (to M.K.), along with funds from the Fralin Life Science Institute of Virginia Tech (to M.B.C.).

We thank Richard Marconi, Frank Yang, and M. Motaleb for providing strains and/or constructs used in these studies. We also thank Ira Schwartz for helpful discussions and sharing microarray data regarding the expression of *Borrelia* genes within ticks and DMCs prior to publication. We are indebted to Ashley Health (Sigma-Aldrich) for his continued assistance with designing the oligonucleotide primers used for our qRT-PCR assays and Amit Luthra for his help predicting the cellular locations of c-di-GMP-regulated proteins.

REFERENCES

1. **Radolf JD, Caimano MJ, Stevenson B, Hu LT.** 2012. Of ticks, mice and men: understanding the dual-host lifestyle of Lyme disease spirochaetes. Nat Rev Microbiol **10:**87–99. http://dx.doi.org/10.1038/nrmicro2714.
2. **Burgdorfer W, Barbour AG, Hayes SF, Benach JL, Grunwaldt E, Davis JP.** 1982. Lyme disease—a tick-borne spirochetosis? Science **216:**1317–1319. http://dx.doi.org/10.1126/science.7043737.
3. **Piesman J, Schwan TG.** 2010. Ecology of *Borreliae* and their arthropod vectors, p 251–278. *In* Samuels DS, Radolf JD (ed), *Borrelia*: molecular biology, host interaction and pathogenesis. Caister Academic Press, Norfolk, United Kingdom.
4. **Balashov YS.** 1972. Blood-sucking ticks (Ixodidae)—vectors of disease of man and animals. Misc Pub Entomol Soc Am **8:**161–376.
5. **Zung JL, Lewengrug S, Mrdzibnska MA, Spielman A.** 1989. Fine structural evidence for the penetration of the Lyme disease spirochete *Borrelia burgdorferi* through the gut and salivary tissues of *Ixodes dammini*. Can J Zool **67:**1737–1748. http://dx.doi.org/10.1139/z89-249.
6. **Dunham-Ems SM, Caimano MJ, Pal U, Wolgemuth CW, Eggers CH, Balic A, Radolf JD.** 2009. Live imaging reveals a biphasic mode of dissemination of *Borrelia burgdorferi* within ticks. J Clin Invest **119:**3652–3665. http://dx.doi.org/10.1172/JCI39401.
7. **Boylan JA, Lawrence KA, Downey JS, Gherardini FC.** 2008. *Borrelia burgdorferi* membranes are the primary targets of reactive oxygen species. Mol Microbiol **68:**786–799. http://dx.doi.org/10.1111/j.1365-2958.2008.06204.x.
8. **Yang X, Smith AA, Williams MS, Pal U.** 2014. A dityrosine network mediated by dual oxidase and peroxidase influences the persistence of Lyme disease pathogens within the vector. J Biol Chem **289:**12813–12822. http://dx.doi.org/10.1074/jbc.M113.538272.
9. **Sonenshine DE, Hynes WL.** 2008. Molecular characterization and related aspects of the innate immune response in ticks. Front Biosci **13:**7046–7063. http://dx.doi.org/10.2741/3209.
10. **Kopacek P, Hajdusek O, Buresova V, Daffre S.** 2010. Tick innate immunity. Adv Exp Med Biol **708:**137–162. http://dx.doi.org/10.1007/978-1-4419-8059-5_8.
11. **Smith AA, Pal U.** 2014. Immunity-related genes in *Ixodes scapularis*—perspectives from genome information. Front Cell Infect Microbiol **4:**116. http://dx.doi.org/10.3389/fcimb.2014.00116.
12. **Pappas CJ, Iyer R, Petzke MM, Caimano MJ, Radolf JD, Schwartz I.** 2011. *Borrelia burgdorferi* requires glycerol for maximum fitness during the tick phase of the enzootic cycle. PLoS Pathog **7:**e1002102. http://dx.doi.org/10.1371/journal.ppat.1002102.
13. **Tilly K, Grimm D, Bueschel DM, Krum JG, Rosa P.** 2004. Infectious cycle analysis of a *Borrelia burgdorferi* mutant defective in transport of chitobiose, a tick cuticle component. Vector Borne Zoonotic Dis **4:**159–168. http://dx.doi.org/10.1089/1530366041210738.
14. **von Lackum K, Stevenson B.** 2005. Carbohydrate utilization by the Lyme borreliosis spirochete, *Borrelia burgdorferi*. FEMS Microbiol Lett **243:**173–179. http://dx.doi.org/10.1016/j.femsle.2004.12.002.
15. **Gherardini F, Boylan JA, Lawrence K, Skare J.** 2010. Metabolism and physiology of *Borrelia*, p 103–138. *In* Samuels DS, Radolf JD (ed), *Borrelia*: molecular biology, host interaction and pathogenesis. Caister Academic Press, Norfolk, United Kingdom.
16. **de Silva AM, Fikrig E.** 1995. Growth and migration of *Borrelia burgdorferi* in *Ixodes* ticks during blood feeding. Am J Trop Med Hyg **53:**397–404.
17. **Samuels DS.** 2011. Gene regulation in *Borrelia burgdorferi*. Annu Rev Microbiol **65:**479–499. http://dx.doi.org/10.1146/annurev.micro.112408.134040.
18. **Xu H, Caimano MJ, Lin T, He M, Radolf JD, Norris SJ, Gherardini F, Wolfe AJ, Yang XF.** 2010. Role of acetyl-phosphate in activation of the Rrp2-RpoN-RpoS pathway in *Borrelia burgdorferi*. PLoS Pathog **6:**e1001104. http://dx.doi.org/10.1371/journal.ppat.1001104.
19. **Dunham-Ems SM, Caimano MJ, Eggers CH, Radolf JD.** 2012. *Borrelia burgdorferi* requires the alternative sigma factor RpoS for dissemination

within the vector during tick-to-mammal transmission. PLoS Pathog **8:**e1002532. http://dx.doi.org/10.1371/journal.ppat.1002532.
20. **Caimano MJ, Eggers CH, Hazlett KR, Radolf JD.** 2004. RpoS is not central to the general stress response in *Borrelia burgdorferi* but does control expression of one or more essential virulence determinants. Infect Immun **72:**6433–6445. http://dx.doi.org/10.1128/IAI.72.11.6433-6445.2004.
21. **Xu Q, Shi Y, Dadhwal P, Liang FT.** 2012. RpoS regulates essential virulence factors remaining to be identified in *Borrelia burgdorferi*. PLoS One **7:**e53212. http://dx.doi.org/10.1371/journal.pone.0053212.
22. **Hubner A, Yang X, Nolen DM, Popova TG, Cabello FC, Norgard MV.** 2001. Expression of *Borrelia burgdorferi* OspC and DbpA is controlled by a RpoN-RpoS regulatory pathway. Proc Natl Acad Sci U S A **98:**12724–12729. http://dx.doi.org/10.1073/pnas.231442498.
23. **Fisher MA, Grimm D, Henion AK, Elias AF, Stewart PE, Rosa PA, Gherardini FC.** 2005. *Borrelia burgdorferi* σ^{54} is required for mammalian infection and vector transmission but not for tick colonization. Proc Natl Acad Sci U S A **102:**5162–5167. http://dx.doi.org/10.1073/pnas.0408536102.
24. **Caimano MJ, Iyer R, Eggers CH, Gonzalez C, Morton EA, Gilbert MA, Schwartz I, Radolf JD.** 2007. Analysis of the RpoS regulon in *Borrelia burgdorferi* in response to mammalian host signals provides insight into RpoS function during the enzootic cycle. Mol Microbiol **65:**1193–1217. http://dx.doi.org/10.1111/j.1365-2958.2007.05860.x.
25. **Gilmore RD, Jr, Howison RR, Schmit VL, Carroll JA.** 2008. *Borrelia burgdorferi* expression of the *bba64*, *bba65*, *bba66*, and *bba73* genes in tissues during persistent infection in mice. Microb Pathog **45:**355–360. http://dx.doi.org/10.1016/j.micpath.2008.08.006.
26. **Liang FT, Nelson FK, Fikrig E.** 2002. Molecular adaptation of *Borrelia burgdorferi* in the murine host. J Exp Med **196:**275–280. http://dx.doi.org/10.1084/jem.20020770.
27. **Ouyang Z, Narasimhan S, Neelakanta G, Kumar M, Pal U, Fikrig E, Norgard MV.** 2012. Activation of the RpoN-RpoS regulatory pathway during the enzootic life cycle of *Borrelia burgdorferi*. BMC Microbiol **12:**44. http://dx.doi.org/10.1186/1471-2180-12-44.
28. **Bunikis J, Tsao J, Luke CJ, Luna MG, Fish D, Barbour AG.** 2004. *Borrelia burgdorferi* infection in a natural population of *Peromyscus leucopus* mice: a longitudinal study in an area where Lyme borreliosis is highly endemic. J Infect Dis **189:**1515–1523. http://dx.doi.org/10.1086/382594.
29. **Crother TR, Champion CI, Whitelegge JP, Aguilera R, Wu XY, Blanco DR, Miller JN, Lovett MA.** 2004. Temporal analysis of the antigenic composition of *Borrelia burgdorferi* during infection in rabbit skin. Infect Immun **72:**5063–5072. http://dx.doi.org/10.1128/IAI.72.9.5063-5072.2004.
30. **Fingerle V, Liegl G, Munderloh U, Wilske B.** 1998. Expression of outer surface proteins A and C of *Borrelia burgdorferi* in *Ixodes ricinus* ticks removed from humans. Med Microbiol Immunol **187:**121–126. http://dx.doi.org/10.1007/s004300050083.
31. **Schwan TG, Piesman J.** 2000. Temporal changes in outer surface proteins A and C of the Lyme disease-associated spirochete, Borrelia burgdorferi, during the chain of infection in ticks and mice. J Clin Microbiol **38:**382–388.
32. **Lahdenne P, Porcella SF, Hagman KE, Akins DR, Popova TG, Cox DL, Katona LI, Radolf JD, Norgard MV.** 1997. Molecular characterization of a 6.6-kilodalton *Borrelia burgdorferi* outer membrane-associated lipoprotein (lp6.6) which appears to be downregulated during mammalian infection. Infect Immun **65:**412–421.
33. **Shi Y, Dadhwal P, Li X, Liang FT.** 2014. BosR functions as a repressor of the *ospAB* operon in *Borrelia burgdorferi*. PLoS One **9:**e109307. http://dx.doi.org/10.1371/journal.pone.0109307.
34. **Caimano MJ, Kenedy MR, Kairu T, Desrosiers DC, Harman M, Dunham-Ems S, Akins DR, Pal U, Radolf JD.** 2011. The hybrid histidine kinase Hk1 is part of a two-component system that is essential for survival of *Borrelia burgdorferi* in feeding *Ixodes scapularis* ticks. Infect Immun **79:**3117–3130. http://dx.doi.org/10.1128/IAI.05136-11.
35. **He M, Ouyang Z, Troxell B, Xu H, Moh A, Piesman J, Norgard MV, Gomelsky M, Yang XF.** 2011. Cyclic-di-GMP is essential for the survival of the Lyme disease spirochete in ticks. PLoS Pathog **7:**e1002133. http://dx.doi.org/10.1371/journal.ppat.1002133.
36. **Kostick JL, Szkotnicki LT, Rogers EA, Bocci P, Raffaelli N, Marconi RT.** 2011. The diguanylate cyclase, Rrp1, regulates critical steps in the enzootic cycle of the Lyme disease spirochetes. Mol Microbiol **81:**219–231. http://dx.doi.org/10.1111/j.1365-2958.2011.07687.x.
37. **Ryjenkov DA, Tarutina M, Moskvin OV, Gomelsky M.** 2005. Cyclic diguanylate is a ubiquitous signaling molecule in bacteria: insights into biochemistry of the GGDEF protein domain. J Bacteriol **187:**1792–1798. http://dx.doi.org/10.1128/JB.187.5.1792-1798.2005.
38. **Mulay VB, Caimano MJ, Iyer R, Dunham-Ems S, Liveris D, Petzke MM, Schwartz I, Radolf JD.** 2009. *Borrelia burgdorferi bba74* is expressed exclusively during tick feeding and is regulated by both arthropod- and mammalian host-specific signals. J Bacteriol **191:**2783–2794. http://dx.doi.org/10.1128/JB.01802-08.
39. **Pollack RJ, Telford SR, Spielman A.** 1993. Standardization of medium for culturing Lyme disease spirochetes. J Clin Microbiol **31:**1251–1255.
40. **Kawabata H, Norris SJ, Watanabe H.** 2004. BBE02 disruption mutants of *Borrelia burgdorferi* B31 have a highly transformable, infectious phenotype. Infect Immun **72:**7147–7154. http://dx.doi.org/10.1128/IAI.72.12.7147-7154.2004.
41. **Samuels DS.** 1995. Electrotransformation of the spirochete *Borrelia burgdorferi*. Electrotransformation protocols for microorganisms. Methods Mol Biol **47:**253–259. http://dx.doi.org/10.1385/0-89603-310-4:253.
42. **Iyer R, Caimano MJ, Luthra A, Axline D, Jr, Corona A, Iacobas DA, Radolf JD, Schwartz I.** 2015. Stage-specific global alterations in the transcriptomes of Lyme disease spirochetes during tick feeding and following mammalian host adaptation. Mol Microbiol **95:**509–538. http://dx.doi.org/10.1111/mmi.12882.
43. **Rogers EA, Terekhova D, Zhang H-M, Hovis KM, Schwartz I, Marconi RT.** 2009. Rrp1, a cyclic-di-GMP-producing response regulator, is an important regulator of *Borrelia burgdorferi* core cellular functions. Mol Microbiol **71:**1551–1573. http://dx.doi.org/10.1111/j.1365-2958.2009.06621.x.
44. **Pitzer JE, Sultan SZ, Hayakawa Y, Hobbs G, Miller MR, Motaleb MA.** 2011. Analysis of the *Borrelia burgdorferi* cyclic-di-GMP-binding protein PlzA reveals a role in motility and virulence. Infect Immun **79:**1815–1825. http://dx.doi.org/10.1128/IAI.00075-11.
45. **Eggers CH, Caimano MJ, Clawson ML, Miller WG, Samuels DS, Radolf JD.** 2002. Identification of loci critical for replication and compatibility of a *Borrelia burgdorferi* cp32 plasmid and use of a cp32-based shuttle vector for the expression of fluorescent reporters in the Lyme disease spirochaete. Mol Microbiol **43:**281–295. http://dx.doi.org/10.1046/j.1365-2958.2002.02758.x.
46. **Caimano MJ, Eggers CH, Gonzalez CA, Radolf JD.** 2005. Alternate sigma factor RpoS is required for the *in vivo*-specific repression of *Borrelia burgdorferi* plasmid lp54-borne *ospA* and *lp6.6* genes. J Bacteriol **187:**7845–7852. http://dx.doi.org/10.1128/JB.187.22.7845-7852.2005.
47. **Akins DR, Bourell KW, Caimano MJ, Norgard MV, Radolf JD.** 1998. A new animal model for studying Lyme disease spirochetes in a mammalian host-adapted state. J Clin Invest **101:**2240–2250. http://dx.doi.org/10.1172/JCI2325.
48. **Laourdakis CD, Merino EF, Neilson AP, Cassera MB.** 2014. Comprehensive quantitative analysis of purines and pyrimidines in the human malaria parasite using ion-pairing ultra-performance liquid chromatography-mass spectrometry. J Chromatogr B Analyt Technol Biomed Life Sci **967:**127–133. http://dx.doi.org/10.1016/j.jchromb.2014.07.012.
49. **Policastro PF, Schwan TG.** 2003. Experimental infection of *Ixodes scapularis* larvae (Acari: Ixodidae) by immersion in low passage cultures of *Borrelia burgdorferi*. J Med Entomol **40:**364–370. http://dx.doi.org/10.1603/0022-2585-40.3.364.
50. **Caimano MJ, Sivasankaran SK, Allard A, Hurley D, Hokamp K, Grassmann AA, Hinton JC, Nally JE.** 2014. A model system for studying the transcriptomic and physiological changes associated with mammalian host-adaptation by *Leptospira interrogans* serovar Copenhageni. PLoS Pathog **10:**e1004004. http://dx.doi.org/10.1371/journal.ppat.1004004.
51. **Warren AS, Aurrecoechea C, Brunk B, Desai P, Emrich S, Giraldo-Calderón GI, Harb O, Hix D, Lawson D, Machi D, Mao C, McClelland M, Nordberg E, Shukla M, Vosshall LB, Wattam AR, Will R, Yoo HS, Sobral B.** 2015. RNA-Rocket: an RNA-Seq analysis resource for infectious disease research. Bioinformatics **31:**1496–1498. http://dx.doi.org/10.1093/bioinformatics/btv002.
52. **Setubal JC, Reis M, Matsunaga J, Haake DA.** 2006. Lipoprotein computational prediction in spirochaetal genomes. Microbiology **152:**113–121. http://dx.doi.org/10.1099/mic.0.28317-0.
53. **Yu CS, Lin CJ, Hwang JK.** 2004. Predicting subcellular localization of proteins for Gram-negative bacteria by support vector machines based on n-peptide compositions. Protein Sci **13:**1402–1406. http://dx.doi.org/10.1110/ps.03479604.
54. **Yu NY, Wagner JR, Laird MR, Melli G, Rey S, Lo R, Dao P, Sahinalp SC, Ester M, Foster LJ, Brinkman FS.** 2010. PSORTb 3.0: improved

protein subcellular localization prediction with refined localization subcategories and predictive capabilities for all prokaryotes. Bioinformatics **26:**1608–1615. http://dx.doi.org/10.1093/bioinformatics/btq249.
55. **Remmert M, Linke D, Lupas AN, Soding J.** 2009. HHomp—prediction and classification of outer membrane proteins. Nucleic Acids Res **37:** W446–W451. http://dx.doi.org/10.1093/nar/gkp325.
56. **Berven FS, Flikka K, Jensen HB, Eidhammer I.** 2004. BOMP: a program to predict integral beta-barrel outer membrane proteins encoded within genomes of Gram-negative bacteria. Nucleic Acids Res **32:**W394–W399. http://dx.doi.org/10.1093/nar/gkh351.
57. **Bagos PG, Liakopoulos TD, Spyropoulos IC, Hamodrakas SJ.** 2004. PRED-TMBB: a web server for predicting the topology of beta-barrel outer membrane proteins. Nucleic Acids Res **32:**W400–W404. http://dx.doi.org/10.1093/nar/gkh417.
58. **Ou YY, Gromiha MM, Chen SA, Suwa M.** 2008. TMBETADISC-RBF: discrimination of beta-barrel membrane proteins using RBF networks and PSSM profiles. Comput Biol Chem **32:**227–231. http://dx.doi.org/10.1016/j.compbiolchem.2008.03.002.
59. **Krogh A, Larsson B, von Heine G, Sonnhammer EL.** 2001. Predicting transmembrane protein topology with a hidden Markov model: application to complete genomes. J Mol Biol **305:**567–580. http://dx.doi.org/10.1006/jmbi.2000.4315.
60. **Kall L, Krogh A, Sonnhammer EL.** 2004. A combined transmembrane topology and signal peptide prediction method. J Mol Biol **338:**1027–1036. http://dx.doi.org/10.1016/j.jmb.2004.03.016.
61. **Bendtsen JD, Nielsen H, von Heijne G, Brunak S.** 2004. Improved prediction of signal peptides: SignalP 3.0. J Mol Biol **340:**783–795. http://dx.doi.org/10.1016/j.jmb.2004.05.028.
62. **Hiller K, Grote A, Scheer M, Munch R, Jahn D.** 2004. PrediSi: prediction of signal peptides and their cleavage positions. Nucleic Acids Res **32:**W375–W379. http://dx.doi.org/10.1093/nar/gkh378.
63. **Chou KC, Shen HB.** 2007. Signal-CF: a subsite-coupled and window-fusing approach for predicting signal peptides. Biochem Biophys Res Commun **357:**633–640. http://dx.doi.org/10.1016/j.bbrc.2007.03.162.
64. **Kyte J, Doolittle RF.** 1982. A simple method for displaying the hydropathic character of a protein. J Mol Biol **157:**105–132. http://dx.doi.org/10.1016/0022-2836(82)90515-0.
65. **Ohnishi J, Piesman J, de Silva AM.** 2001. Antigenic and genetic heterogeneity of *Borrelia burgdorferi* populations transmitted by ticks. Proc Natl Acad Sci U S A **98:**670–675. http://dx.doi.org/10.1073/pnas.98.2.670.
66. **Tilly K, Krum JG, Bestor A, Jewett MW, Grimm D, Bueschel D, Byram R, Dorward D, Vanraden MJ, Stewart P, Rosa P.** 2006. *Borrelia burgdorferi* OspC protein required exclusively in a crucial early stage of mammalian infection. Infect Immun **74:**3554–3564. http://dx.doi.org/10.1128/IAI.01950-05.
67. **Bockenstedt LK, Gonzalez D, Mao J, Li M, Belperron AA, Haberman A.** 2014. What ticks do under your skin: two-photon intravital imaging of *Ixodes scapularis* feeding in the presence of the Lyme disease spirochete. Yale J Biol Med **87:**3–13.
68. **Bockenstedt LK, Gonzalez DG, Haberman AM, Belperron AA.** 2012. Spirochete antigens persist near cartilage after murine Lyme borreliosis therapy. J Clin Invest **122:**2652–2660. http://dx.doi.org/10.1172/JCI58813.
69. **Harman MW, Dunham-Ems SM, Caimano MJ, Belperron AA, Bockenstedt LK, Fu HC, Radolf JD, Wolgemuth CW.** 2012. The heterogeneous motility of the Lyme disease spirochete in gelatin mimics dissemination through tissue. Proc Natl Acad Sci U S A **109:**3059–3064. http://dx.doi.org/10.1073/pnas.1114362109.
70. **Bockenstedt LK, Liu N, Schwartz I, Fish D.** 2006. MyD88 deficiency enhances acquisition and transmission of *Borrelia burgdorferi* by *Ixodes scapularis* ticks. Infect Immun **74:**2154–2160. http://dx.doi.org/10.1128/IAI.74.4.2154-2160.2006.
71. **Pedra JH, Narasimhan S, Deponte K, Marcantonio N, Kantor FS, Fikrig E.** 2006. Disruption of the salivary protein 14 in *Ixodes scapularis* nymphs and impact on pathogen acquisition. Am J Trop Med Hyg **75:**677–682.
72. **Coleman JL, Sellati TJ, Testa JE, Kew RR, Furie MB, Benach JL.** 1995. *Borrelia burgdorferi* binds plasminogen, resulting in enhanced penetration of endothelial monolayers. Infect Immun **63:**2478–2484.
73. **Balashov YS, Grigoryeva LA.** 2003. Cytological changes in the midgut of tick females of the genus *Ixodes* during and after feeding. Dokl Biol Sci **393:**527–530. http://dx.doi.org/10.1023/B:DOBS.0000010314.97335.2c.
74. **Franta Z, Frantova H, Konvickova J, Horn M, Sojka D, Mares M, Kopacek P.** 2010. Dynamics of digestive proteolytic system during blood feeding of the hard tick *Ixodes ricinus*. Parasites Vectors **3:**119. http://dx.doi.org/10.1186/1756-3305-3-119.
75. **Croucher NJ, Fookes MC, Perkins TT, Turner DJ, Marguerat SB, Keane T, Quail MA, He M, Assefa S, Bähler J, Kingsley RA, Parkhill J, Bentley SD, Dougan G, Thomson NR.** 2009. A simple method for directional transcriptome sequencing using Illumina technology. Nucleic Acids Res **37:**e148. http://dx.doi.org/10.1093/nar/gkp811.
76. **Croucher NJ, Thomson NR.** 2010. Studying bacterial transcriptomes using RNA-seq. Curr Opin Microbiol **13:**619–624. http://dx.doi.org/10.1016/j.mib.2010.09.009.
77. **Porcella SF, Fitzpatrick CA, Bono JL.** 2000. Expression and immunological analysis of the plasmid-borne *mlp* genes of *Borrelia burgdorferi* B31. Infect Immun **68:**4992–5001. http://dx.doi.org/10.1128/IAI.68.9.4992-5001.2000.
78. **Caimano MJ, Yang X, Popova TG, Clawson ML, Akins DR, Norgard MV, Radolf JD.** 2000. Molecular and evolutionary characterization of the cp32/18 family of supercoiled plasmids in *Borrelia burgdorferi* 297. Infect Immun **68:**1574–1586. http://dx.doi.org/10.1128/IAI.68.3.1574-1586.2000.
79. **Brisson D, Zhou W, Jutras BL, Casjens S, Stevenson B.** 2013. Distribution of cp32 prophages among Lyme disease-causing spirochetes and natural diversity of their lipoprotein-encoding *erp* loci. Appl Environ Microbiol **79:**4115–4128. http://dx.doi.org/10.1128/AEM.00817-13.
80. **Kraiczy P, Stevenson B.** 2013. Complement regulator-acquiring surface proteins of *Borrelia burgdorferi*: structure, function and regulation of gene expression. Ticks Tick-Borne Dis **4:**26–34. http://dx.doi.org/10.1016/j.ttbdis.2012.10.039.
81. **Bhattacharjee A, Oeemig JS, Kolodziejczyk R, Meri T, Kajander T, Lehtinen MJ, Iwai H, Jokiranta TS, Goldman A.** 2013. Structural basis for complement evasion by Lyme disease pathogen *Borrelia burgdorferi*. J Biol Chem **288:**18685–18695. http://dx.doi.org/10.1074/jbc.M113.459040.
82. **Zhang X, Yang X, Kumar M, Pal U.** 2009. BB0323 function is essential for *Borrelia burgdorferi* virulence and persistence through tick-rodent transmission cycle. J Infect Dis **200:**1318–1330. http://dx.doi.org/10.1086/605846.
83. **Kariu T, Yang X, Marks CB, Zhang X, Pal U.** 2013. Proteolysis of BB0323 results in two polypeptides that impact physiologic and infectious phenotypes in *Borrelia burgdorferi*. Mol Microbiol **88:**510–522. http://dx.doi.org/10.1111/mmi.12202.
84. **Promnares K, Kumar M, Shroder DY, Zhang X, Anderson JF, Pal U.** 2009. *Borrelia burgdorferi* small lipoprotein Lp6.6 is a member of multiple protein complexes in the outer membrane and facilitates pathogen transmission from ticks to mice. Mol Microbiol **74:**112–125. http://dx.doi.org/10.1111/j.1365-2958.2009.06853.x.
85. **Bono JL, Tilly K, Stevenson B, Hogan D, Rosa P.** 1998. Oligopeptide permease in *Borrelia burgdorferi*: putative peptide-binding components encoded by both chromosomal and plasmid loci. Microbiology **144**(Pt 4)**:**1033–1044. http://dx.doi.org/10.1099/00221287-144-4-1033.
86. **Medrano MS, Ding Y, Wang XG, Lu P, Coburn J, Hu LT.** 2007. Regulators of expression of the oligopeptide permease A proteins of *Borrelia burgdorferi*. J Bacteriol **189:**2653–2659. http://dx.doi.org/10.1128/JB.01760-06.
87. **Cerveny L, Straskova A, Dankova V, Hartlova A, Ceckova M, Staud F, Stulik J.** 2013. Tetratricopeptide repeat motifs in the world of bacterial pathogens: role in virulence mechanisms. Infect Immun **81:**629–635. http://dx.doi.org/10.1128/IAI.01035-12.
88. **Roberts DM, Caimano M, McDowell J, Theisen M, Holm A, Orff E, Nelson D, Wikel S, Radolf J, Marconi RT.** 2002. Environmental regulation and differential production of members of the Bdr protein family of *Borrelia burgdorferi*. Infect Immun **70:**7033–7041. http://dx.doi.org/10.1128/IAI.70.12.7033-7041.2002.
89. **Roberts DM, Carlyon JA, Theisen M, Marconi RT.** 2000. The *bdr* gene families of the Lyme disease and relapsing fever spirochetes: potential influence on biology, pathogenesis, and evolution. Emerg Infect Dis **6:**110–122. http://dx.doi.org/10.3201/eid0602.000203.
90. **Roberts DM, Theisen M, Marconi RT.** 2000. Analysis of the cellular localization of Bdr paralogs in *Borrelia burgdorferi*, a causative agent of Lyme disease: evidence for functional diversity. J Bacteriol **182:**4222–4226. http://dx.doi.org/10.1128/JB.182.15.4222-4226.2000.
91. **Gutierrez JA, Csonka LN.** 1995. Isolation and characterization of adenylate kinase (adk) mutations in *Salmonella typhimurium* which block

the ability of glycine betaine to function as an osmoprotectant. J Bacteriol **177:**390–400.
92. **Thein M, Bonde M, Bunikis I, Denker K, Sickmann A, Bergström S, Benz R.** 2012. DipA, a pore-forming protein in the outer membrane of Lyme disease spirochetes exhibits specificity for the permeation of dicarboxylates. PLoS One **7:**e36523. http://dx.doi.org/10.1371/journal.pone.0036523.
93. **Barcena-Uribarri I, Thein M, Barbot M, Sans-Serramitjana E, Bonde M, Mentele R, Lottspeich F, Bergstrom S, Benz R.** 2014. Study of the protein complex, pore diameter, and pore-forming activity of the *Borrelia burgdorferi* P13 porin. J Biol Chem **289:**18614–18624. http://dx.doi.org/10.1074/jbc.M113.539528.
94. **Mulay V, Caimano MJ, Liveris D, Desrosiers DC, Radolf JD, Schwartz I.** 2007. *Borrelia burgdorferi* BBA74, a periplasmic protein associated with the outer membrane, lacks porin-like properties. J Bacteriol **189:**2063–2068. http://dx.doi.org/10.1128/JB.01239-06.
95. **Van Laar TA, Lin YH, Miller CL, Karna SL, Chambers JP, Seshu J.** 2012. Effect of levels of acetate on the mevalonate pathway of *Borrelia burgdorferi*. PLoS One **7:**e38171. http://dx.doi.org/10.1371/journal.pone.0038171.
96. **Tilly K, Elias AF, Errett J, Fischer E, Iyer R, Schwartz I, Bono JL, Rosa P.** 2001. Genetics and regulation of chitobiose utilization in *Borrelia burgdorferi*. J Bacteriol **183:**5544–5553. http://dx.doi.org/10.1128/JB.183.19.5544-5553.2001.
97. **Hoon-Hanks LL, Morton EA, Lybecker MC, Battisti JM, Scott Samuels D, Drecktrah D.** 2012. *Borrelia burgdorferi malQ* mutants utilize disaccharides and traverse the enzootic cycle. FEMS Immunol Med Microbiol **66:**157–165. http://dx.doi.org/10.1111/j.1574-695X.2012.00996.x.
98. **Py B, Barras F.** 2010. Building Fe-S proteins: bacterial strategies. Nat Rev Microbiol **8:**436–446. http://dx.doi.org/10.1038/nrmicro2356.
99. **Kashyap DR, Rompca A, Gaballa A, Helmann JD, Chan J, Chang CJ, Hozo I, Gupta D, Dziarski R.** 2014. Peptidoglycan recognition proteins kill bacteria by inducing oxidative, thiol, and metal stress. PLoS Pathog **10:**e1004280. http://dx.doi.org/10.1371/journal.ppat.1004280.
100. **Posey JE, Gherardini FC.** 2000. Lack of a role for iron in the Lyme disease pathogen. Science **288:**1651–1653. http://dx.doi.org/10.1126/science.288.5471.1651.
101. **Wang P, Lutton A, Olesik J, Vali H, Li X.** 2012. A novel iron- and copper-binding protein in the Lyme disease spirochaete. Mol Microbiol **86:**1441–1451. http://dx.doi.org/10.1111/mmi.12068.
102. **Freedman JC, Rogers EA, Kostick JL, Zhang H, Iyer R, Schwartz I, Marconi RT.** 2010. Identification and molecular characterization of a cyclic-di-GMP effector protein, PlzA (BB0733): additional evidence for the existence of a functional cyclic-di-GMP regulatory network in the Lyme disease spirochete, *Borrelia burgdorferi*. FEMS Immunol Med Microbiol **58:**285–294. http://dx.doi.org/10.1111/j.1574-695X.2009.00635.x.
103. **Novak EA, Sultan SZ, Motaleb MA.** 2014. The cyclic-di-GMP signaling pathway in the Lyme disease spirochete, *Borrelia burgdorferi*. Front Cell Infect Microbiol **4:**56. http://dx.doi.org/10.3389/fcimb.2014.00056.
104. **Jutras BL, Chenail AM, Rowland CL, Carroll D, Miller MC, Bykowski T, Stevenson B.** 2013. Eubacterial SpoVG homologs constitute a new family of site-specific DNA-binding proteins. PLoS One **8:**e66683. http://dx.doi.org/10.1371/journal.pone.0066683.
105. **Miller CL, Karna SL, Seshu J.** 2013. *Borrelia* host adaptation regulator (BadR) regulates *rpoS* to modulate host adaptation and virulence factors in *Borrelia burgdorferi*. Mol Microbiol **88:**105–124. http://dx.doi.org/10.1111/mmi.12171.
106. **Boardman BK, He M, Ouyang Z, Xu H, Pang X, Yang XF.** 2008. Essential role of the response regulator Rrp2 in the infectious cycle of *Borrelia burgdorferi*. Infect Immun **76:**3844–3853. http://dx.doi.org/10.1128/IAI.00467-08.
107. **Yang XF, Alani SM, Norgard MV.** 2003. The response regulator Rrp2 is essential for the expression of major membrane lipoproteins in *Borrelia burgdorferi*. Proc Natl Acad Sci U S A **100:**11001–11006. http://dx.doi.org/10.1073/pnas.1834315100.
108. **Weening EH, Parveen N, Trzeciakowski JP, Leong JM, Hook M, Skare JT.** 2008. *Borrelia burgdorferi* lacking *dbpBA* exhibits an early survival defect during experimental infection. Infect Immun **76:**5694–5705. http://dx.doi.org/10.1128/IAI.00690-08.
109. **Hyde JA, Weening EH, Chang M, Trzeciakowski JP, Höök M, Cirillo JD, Skare JT.** 2011. Bioluminescent imaging of *Borrelia burgdorferi in vivo* demonstrates that the fibronectin-binding protein BBK32 is required for optimal infectivity. Mol Microbiol **82:**99–113. http://dx.doi.org/10.1111/j.1365-2958.2011.07801.x.
110. **Shi Y, Xu Q, McShan K, Liang FT.** 2008. Both decorin-binding proteins A and B are critical for the overall virulence of *Borrelia burgdorferi*. Infect Immun **76:**1239–1246. http://dx.doi.org/10.1128/IAI.00897-07.
111. **Fortune DE, Lin YP, Deka RK, Groshong AM, Moore BP, Hagman KE, Leong JM, Tomchick DR, Blevins JS.** 2014. Identification of lysine residues in the *Borrelia burgdorferi* DbpA adhesin required for murine infection. Infect Immun **82:**3186–3198. http://dx.doi.org/10.1128/IAI.02036-14.
112. **Moriarty TJ, Shi M, Lin YP, Ebady R, Zhou H, Odisho T, Hardy PO, Salman-Dilgimen A, Wu J, Weening EH, Skare JT, Kubes P, Leong J, Chaconas G.** 2012. Vascular binding of a pathogen under shear force through mechanistically distinct sequential interactions with host macromolecules. Mol Microbiol **86:**1116–1131. http://dx.doi.org/10.1111/mmi.12045.
113. **Sze CW, Zhang K, Kariu T, Pal U, Li C.** 2012. *Borrelia burgdorferi* needs chemotaxis to establish infection in mammals and to accomplish its enzootic cycle. Infect Immun **80:**2485–2492. http://dx.doi.org/10.1128/IAI.00145-12.
114. **Shih CM, Chao LL, Yu CP.** 2002. Chemotactic migration of the Lyme disease spirochete (*Borrelia burgdorferi*) to salivary gland extracts of vector ticks. Am J Trop Med Hyg **66:**616–621.
115. **He M, Zhang JJ, Ye M, Lou Y, Yang XF.** 2014. Cyclic di-GMP receptor PlzA controls virulence gene expression through RpoS in *Borrelia burgdorferi*. Infect Immun **82:**445–452. http://dx.doi.org/10.1128/IAI.01238-13.
116. **Sze CW, Smith A, Choi YH, Yang X, Pal U, Yu A, Li C.** 2013. Study of the response regulator Rrp1 reveals its regulatory role in chitobiose utilization and virulence of *Borrelia burgdorferi*. Infect Immun **81:**1775–1787. http://dx.doi.org/10.1128/IAI.00050-13.
117. **Eggers CH, Caimano MJ, Malizia RA, Kariu T, Cusack B, Desrosiers DC, Hazlett KR, Claiborne A, Pal U, Radolf JD.** 2011. The coenzyme A disulphide reductase of *Borrelia burgdorferi* is important for rapid growth throughout the enzootic cycle and essential for infection of the mammalian host. Mol Microbiol **82:**679–697. http://dx.doi.org/10.1111/j.1365-2958.2011.07845.x.
118. **Patton TG, Brandt KS, Nolder C, Clifton DR, Carroll JA, Gilmore RD.** 2013. *Borrelia burgdorferi bba66* gene inactivation results in attenuated mouse infection by tick transmission. Infect Immun **81:**2488–2498. http://dx.doi.org/10.1128/IAI.00140-13.
119. **Patton TG, Dietrich G, Dolan MC, Piesman J, Carroll JA, Gilmore RD, Jr.** 2011. Functional analysis of the *Borrelia burgdorferi bba64* gene product in murine infection *via* tick infestation. PLoS One **6:**e19536. http://dx.doi.org/10.1371/journal.pone.0019536.
120. **Bergstrom S, Zuckert WR.** 2010. Structure, function and biogenesis of the *Borrelia* cell envelope, p 139–166. *In* Samuels DS, Radolf JD (ed), *Borrelia*: molecular biology, host interaction and pathogenesis. Caister Academic Press, Norfolk, United Kingdom.
121. **Fraser CM, Casjens S, Huang WM, Sutton GG, Clayton R, Lathigra R, White O, Ketchum KA, Dodson R, Hickey EK, Gwinn M, Dougherty B, Tomb JF, Fleischmann RD, Richardson D, Peterson J, Kerlavage AR, Quackenbush J, Salzberg S, Hanson M, van Vugt R, Palmer N, Adams MD, Gocayne J, Weidman J, Utterback T, Watthey L, McDonald L, Artiach P, Bowman C, Garland S, Fujii C, Cotton MD, Horst K, Roberts K, Hatch B, Smith HO, Venter JC.** 1997. Genomic sequence of a Lyme disease spirochaete, *Borrelia burgdorferi*. Nature **390:**580–586. http://dx.doi.org/10.1038/37551.
122. **Schreuder LJ, Carroll P, Muwanguzi-Karugaba J, Kokoczka R, Brown AC, Parish T.** 2015. *Mycobacterium tuberculosis* H37Rv has a single nucleotide polymorphism in PhoR which affects cell wall hydrophobicity and gene expression. Microbiology **161:**765–773. http://dx.doi.org/10.1099/mic.0.000036.
123. **Kreamer NN, Costa F, Newman DK.** 2015. The ferrous iron-responsive BqsRS two-component system activates genes that promote cationic stress tolerance. mBio **6**(2):e02549. http://dx.doi.org/10.1128/mBio.02549-14.
124. **Nielsen PK, Andersen AZ, Mols M, van der Veen S, Abee T, Kallipolitis BH.** 2012. Genome-wide transcriptional profiling of the cell envelope stress response and the role of LisRK and CesRK in *Listeria monocytogenes*. Microbiology **158:**963–974. http://dx.doi.org/10.1099/mic.0.055467-0.
125. **Datta P, Ravi J, Guerrini V, Chauhan R, Neiditch MB, Shell SS, Fortune SM, Hancioglu B, Igoshin O, Gennaro ML.** 21 April 2015. The Psp system of Mycobacterium tuberculosis integrates envelope stress

sensing and envelope preserving functions. Mol Microbiol. http://dx.doi.org/10.1111/mmi.13037.
126. **Hunke S, Keller R, Muller VS.** 2012. Signal integration by the Cpx-envelope stress system. FEMS Microbiol Lett **326:**12–22. http://dx.doi.org/10.1111/j.1574-6968.2011.02436.x.
127. **Vogt SL, Raivio TL.** 2012. Just scratching the surface: an expanding view of the Cpx envelope stress response. FEMS Microbiol Lett **326:**2–11. http://dx.doi.org/10.1111/j.1574-6968.2011.02406.x.
128. **Dalebroux ZD, Miller SI.** 2014. Salmonellae PhoPQ regulation of the outer membrane to resist innate immunity. Curr Opin Microbiol **17:**106–113. http://dx.doi.org/10.1016/j.mib.2013.12.005.
129. **Romling U, Galperin MY, Gomelsky M.** 2013. Cyclic di-GMP: the first 25 years of a universal bacterial second messenger. Microbiol Mol Biol Rev **77:**1–52. http://dx.doi.org/10.1128/MMBR.00043-12.
130. **Sultan SZ, Sekar P, Zhao X, Manne A, Liu J, Wooten RM, Motaleb MA.** 2015. Motor rotation is essential for the formation of the periplasmic flagellar ribbon, cellular morphology, and *Borrelia burgdorferi* persistence within *Ixodes scapularis* tick and murine hosts. Infect Immun **83:**1765–1777. http://dx.doi.org/10.1128/IAI.03097-14.
131. **Bauer W, Luthra A, Zhu G, Radolf JD, Malkowski M, Caimano MJ.** 2105. Structural characterization of the *Borrelia burgdorferi* hybrid histidine kinase Hk1 periplasmic sensor: a novel system for sensing small molecules associated with tick feeding.
132. **Herrou J, Bompard C, Wintjens R, Dupré E, Willery E, Villeret V, Locht C, Antoine R, Jacob-Dubuisson F.** 2010. Periplasmic domain of the sensor-kinase BvgS reveals a new paradigm for the Venus flytrap mechanism. Proc Natl Acad Sci U S A **107:**17351–17355. http://dx.doi.org/10.1073/pnas.1006267107.
133. **Dupré E, Herrou J, Lensink MF, Wintjens R, Vagin A, Lebedev A, Crosson S, Villeret V, Locht C, Antoine R, Jacob-Dubuisson F.** 2015. Virulence regulation with Venus flytrap domains: structure and function of the periplasmic moiety of the sensor-kinase BvgS. PLoS Pathog **11:**e1004700. http://dx.doi.org/10.1371/journal.ppat.1004700.
134. **Cheung J, Le-Khac M, Hendrickson WA.** 2009. Crystal structure of a histidine kinase sensor domain with similarity to periplasmic binding proteins. Proteins **77:**235–241. http://dx.doi.org/10.1002/prot.22485.
135. **Simm R, Morr M, Remminghorst U, Andersson M, Romling U.** 2009. Quantitative determination of cyclic diguanosine monophosphate concentrations in nucleotide extracts of bacteria by matrix-assisted laser desorption/ionization-time-of-flight mass spectrometry. Anal Biochem **386:**53–58. http://dx.doi.org/10.1016/j.ab.2008.12.013.
136. **National Research Council**. 2011. Guide for the care and use of laboratory animals, 8th ed. National Academies Press, Washington, DC.